The 13th Symposium on Polar Science

15 – 18 November 2022

National Institute of Polar Research
Research Organization of Information and Systems

Session IA

Arctic Research

Program and Abstracts

Conveners
Hiroshi Miyaoka, Teruo Aoki, Kentaro Nishimoto, Hiroyuki Enomoto, and Hironori Yabuki (NIPR)

【IA】Arctic Research

Scopes

This session invites presentations from a wide range of topics related to the Arctic, including all disciplines of natural sciences, engineering, humanities and social sciences.
The Arctic is experiencing rapid environmental and amplified climatic changes, creating significant challenges for people living in this region and various impacts around the globe. We have been trying to elucidate the whole picture of these changes in the Arctic and their phenomena, but many open questions still remain. The Arctic change also has impacts on the global climate as well as ecosystems and human societies in higher-middle latitudes, which is also a scope of the session.
We welcome the contributions on the latest findings on the ongoing change in the Arctic, as well as its past change and perspectives on future change, improved understanding of processes and mechanisms, its impact on our society.

Conveners : **Hiroshi Miyaoka, Teruo Aoki, Kentaro Nishimoto, Hiroyuki Enomoto, and Hironori Yabuki (NIPR)**

Real-time Oral presentations (13:00 – 15:35)

Date: Thu. 17 November

Chair: Hiroyuki Enomoto and Hiroshi Miyaoka (NIPR)			
IAo1	**13:00 - 13:15**	A brief review of current sea ice numerical models and sea ice modelling through two-way ocean-sea ice coupled model	*XINGKUN XU(The University of Tokyo), Takehiko Nose(The University of Tokyo), Yasushi Fujiwara(The University of Tokyo). Tsubasa Kodaira(The University of Tokyo), Takuji Waseda(The University of Tokyo)
IAo2	**13:15 - 13:30**	Estimation of the Arctic sea ice thickness based on the backward tracking analysis	*Noriaki Kimura(The University of Tokyo), Hiroyasu Hasumi(The University of Tokyo)
IAo3	**13:30 - 13:45**	Prediction of summer Arctic sea-ice distribution with a statistical method	*Motomu Oyama(NIPR), Hajime Yamaguchi(NIPR), Noriaki Kimura (The University of Tokyo)
IAo4	**13:45 - 14:00**	Modification of Atlantic Water in the Barent Sea	*Takao Kawasaki(The University of Tokyo), Yoshiki Komuro(JAMSTEC), Jun One(JAMSTEC), Hitoyasu Hasumi(The University of Tokyo/JAMSTEC)
	14:00 - 14:20	Break	
IAo5	**14:20 - 14:35**	Overview of the R/V Mirai Arctic Ocean cruise in 2022	*Motoyo Itoh(JAMSTEC), Jonaotaro Onodeara(JAMSTEC),Mariko Hatta(JAMSTEC), Shigeto Nishino(JAMSTEC), Amane Fujiwara(JAMSTEC), Eiji Watanabe(JAMSTEC),Akihiko Murata(JAMSTEC),Takashi Kikuchi(JAMSTEC)
IAo6	**14:35 - 14:50**	Ocean wave observation by multiple drifting buoys in Beaufort Sea of the Arctic Ocean	*Tomotaka Katsuno(The University of Tokyo), Tsubasa Kodaira(The University of Tokyo), Takehiko Nose(The University of Tokyo), Uchiyama Ryosuke(The University of Tokyo),Takuji Waseda(The University of Tokyo/JAMSTEC)

IAo7	**14:50 - 15:05**	An overview of multi-OpenMetBuoy wave observations in the melting Greenland Sea marginal ice zone	*Takehiko Nose(The University of Tokyo), Mario Hoppmann(Alfred Wegener Institute),Jean Rabault(The Norwegian Meteorological Institute), Takuji Waseda(The University of Tokyo), Tsubasa Kodaira(The University of Tokyo),Tomotaka Tatsuno(The University of Tokyo),Christian Haas(Alfred Wegener Institute)
IAo8	**15:05 - 15:20**	Distinct sources of variability in the euphotic depth within the Arctic seas	*Taka Hirata(Hokkaido University),Keiko Sato(Hokkaido University),Victor Kuwahara(Soka University),Joji Ishizaka(Nagoya University),Toru Hirawake(NIPR), Taiga Nakayana(JAXA), Hiroshi Murakami(JAXA)
IAo9	**15:20 - 15:35**	Data Management of Arctic Project in Japan	*Hironori Yabuki(NIPR), Takeshi Sugimura(NIPR), Takeshi Terui(NIPR)
Chair: Hironori Yabuki (NIPR)			
	16:00 - 16:30	3-minute poster appeal (10 short talks of IAp1 – IAp10)	
	16:30 - 17:30	Poster session core time	

Real-time Poster presentations (16:00 – 17:30)

Date: Thu. 17 November

IAp1	Improvement of sea ice thickness measurement method using the shipborne Electro-Magnetic Inductive device	*Kosuke Kawamura(Kitami Institute of Technology), Kazutaka Tateyama(Kitami Institute of Technology)
IAp2	Response of Eurasian Temperature to Barents–Kara Sea Ice: Evaluation by Multi-Model Seasonal Predictions	*Kensuke Komatsu(MRI), Yuhei Takaya(MRI), Takahiro Toyoda(MRI), Hiroyasu Hasumi(The University of Tokyo)
IAp3	Two new species of basidiomycetous yeast Mrakia sp. isolated from Ward Hunt Lake in the Canadian High Arctic	*Masaharu Tsuji(National Institute of Technology, Asahikawa College), Yukiko Tanabe(NIPR),Warwick Vincent(Université Laval), Masaki Uchida(NIPR)
IAp4	Co-occurrence patterns of soil microbial communities in the low Arctic tundra are affected by the vegetation coverage	*Shu Kuan Wong(NIPR), Yingshun Cui(Division of Life Science & Plant Molecular Biology and Biotechnology Research Center, Korea), Seong-Jun Chun(National Institute of Ecology, Korea),Ryo Kaneko(Bioinsight),Shota Masumoto(Yokohama National University), Ryo Kitagawa(Forestry and Forest Products Research Institute), Akira Mori(Yokohama National University),Masaki Uchida(NIPR)
IAp5	Drone survey of Qaanaaq Glacier, northwestern Greenland, for precise DEM construction and for mapping supraglacial streams	*Shinta Ukai(Hokkaido University), Shin Sugita(Hokkaido University), Ken Kondo(Hokkaido University)
IAp6	Changes in stripe patterns in dark regions on the southwestern Greenland Ice Sheet	*Akane Uruma(Chiba University), Nozomu Takeuchi(Chiba University)
IAp7	Recent activities of the ArCS II Research Infrastructure: Earth Observation Satellite Data	*Rigen Shimada(JAXA), Kazuki Nakata(JAXA), Misako Kachi(JAXA), Takeo Tadono(JAXA), Hiroshi Murakami(JAXA), Eri Yoshizawa(JAXA), Yukio Kurihara(JAXA)

IAp8	Testing of alternative data for generating the JASMES long-term snow cover extent product	*Masahiro Hori(University of Toyama),Masashi Niwano(MRI/NIPR), Rigen Shimada(JAXA/MRI), Teruo Aoki(NIPR/MRI)
IAp9	Fast computation of Arctic Sea Route Search Systems using GPUs	*Takeshi Sugimura(NIPR), Hironori Yabuki(NIPR), Hijime Yamaguchi(NIPR)
IAp10	Educational Practices using Polar Sea Ice Data for High School Science and Mathematics Classes	*Yoshihiro Niwa(NIPR), Takashi Ishibashi(Secondary School attached to the Faculty of Education, the University of Tokyo),Akiko Mohri(NIPR), Hironori Yabuki(NIPR)

Real-time Oral presentations (09:30 – 11:15)

Date: Fri. 18 November

Chair: Teruo Aoki and Kentaro Nishimoto (NIPR) (NIPR)			
IAo10	**9:30 - 10:00**	Relationship between Anthropogenic Aerosol Increase and Arctic Surface Cooling in mid-20th Century	*Takuro Aizawa(NIPR / MRI), Naga Oshima(MRI), Seiji Yukimoto(MRI)
IAo11	**10:00 - 10:15**	Surface melt at SIGMA-B site in Qaanaaq Ice Cap, northwestern Greenland triggered by radiant fluxes in the 2015, 2019, 2020 summers	*Motoshi Nishimura(NIPR), Teruo Aoki(NIPR), Masashi Niwano(MRI), Sumito Matoba(ILTS, Hokkaido University), Tomonori Tanikawa(MRI), Satoru Yamaguchi(National Research Institute for Earth Science and Disaster Resilience), Tetsuhide Yamazaki(Avangnaq Arctic Project)
IAo12	**10:15 - 10:30**	Mass loss of Qaanaaq Ice Cap in northwestern Greenland from 2012 to 2022	*Kaho Watanabe(ILTS, Hokkaido University), Ken Kondo(ILTS, Hokkaido University), Shin Sugiyama(ILTS, Hokkaido University)
IAo13	**10:30 - 10:45**	Ground penetrating radar survey on Qaanaaq Glacier in northwestern Greenland	*Ken Sato(Hokkaido University),Shin Sugiyama(Hokkaido University)
IAo14	**10:45 - 11:00**	Meltwater discharge from Qaanaaq Glacier in the summer 2022	*Takuro Imazu(ILTS,Hokkaido University), Ken Kondo(ILTS,Hokkaido University), Shin Sugiyama(ILTS,Hokkaido University)
IAo15	**11:00 - 11:15**	Russia's international Arctic policy after the invasion of Ukraine : Experts' voices in the domestic media	*Marina LOMAEVA(Arctic Research Center, Hokkaido University), Fujio Ohnishi(Arctic Research Center, Hokkaido University)

A brief review of current sea ice numerical models and sea ice modelling through two-way ocean-sea ice coupled model

Xingkun Xu[1], Yasushi Fujiwara[1], Takehiko Nose[1], Tsubasa Kodaira[1], and Takuji Waseda[1]
[1]*Graduate School of Frontier Sciences, The University of Tokyo*

Prompted by the uncompromising effects of global climate change on the polar seas, in particular Arctic sea ice, there has been a staggering resurgence of interest in how ocean currents and waves are affected by sea ice fields of various kinds and how the sea ice that constitutes those ice fields is altered by the oceanic impacts. However, due to the lack of physical and dynamical knowledge related to the ocean-sea ice interaction processes and the limitations of current numerical modelling skills, in the most recent decades, accurate representation of the complex ocean-sea ice modelling still requires continuous efforts. In particular, the rapid decline of the sea ice cover in Arctic summer has contributed to increasing areas of ice-free ocean. This provides sufficient fetch for ocean waves with ongoing development.

Before investigating how ocean currents and/or waves interact with the sea ice through modelling, a comprehensive review related to the sea ice modelling is required. Here, we briefly reviewed current sea ice and coupled sea ice models. We found current sea ice models are developed based on three different theoretical models (i.e., thermal model with examples as D. L. Feltham et al (2006) *GRL*, E. C. Hunke et al (2010) *JGR: Oceans*, dynamical models with case as M. A. Hopkins et al (2004) *JRG: Oceans*, and thickness models such as W. H. Lipscomb et al (2001) *JGR: Oceans*). Currently, based on three theoretical models introduced above, different sea ice models have been constructed for operational forecasting, such as Los Alamos sea ice model (CICE) developed by U.S. Department of Energy (DOE) during the mid-1990s utilizing Arakawa-B grid (E. C. Hunke et al (2010) *Ocean Modelling*), Louvain-la-Neuve sea ice model (LIM) developed by the Centro Euro-Mediterraneo sui Cambiamenti Climatici utilizing the Arakawa-C grid (T. Fichefet and M. A. Maqueda (1997) *JGR: Oceans*), and sea ice simulator (SIS) developed by the U.S. Geophysical Fluid Dynamics Laboratory (GFDL) (W. Michael (2000) *JAOT*).

In this study, we, following A. Adcroft (2019) *JAMES,* applied the MOM6-S IS2 model for a sea ice hindcast in 2014 for studying the interaction between ocean currents and sea ice, particularly in Arctic. For future plan, the MOM6-SIS2 model would be adopted for a regional ocean-sea ice two-way coupled numerical model construction and further consider the impacts of ocean waves on the sea ice and oceanic field through the updated regional model. This, hopefully, can be utilized for future operational forecasting during the Arctic observation cruise.

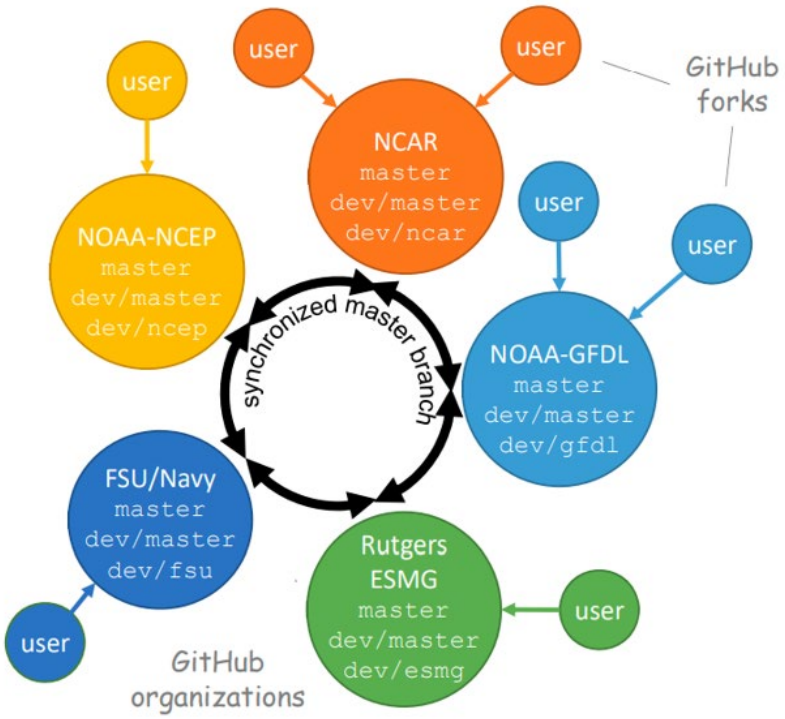

Fig1. Schematic illustration of the MOM6-SIS2 coupled numerical model from Adcroft et al. (2019) *JAMES*

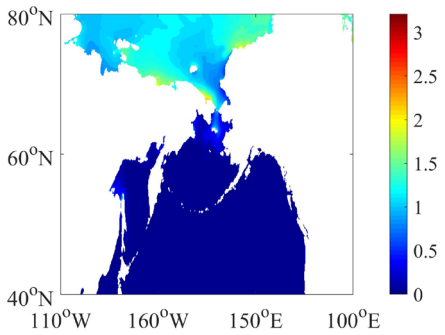

Fig2. Monthly average of sea ice thickness in January of 2014

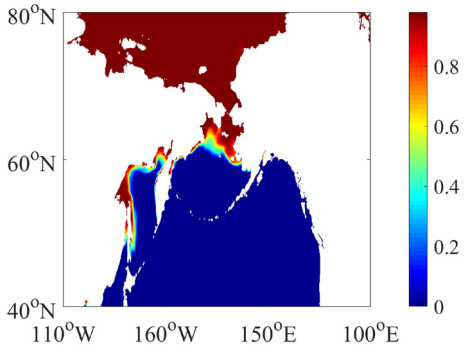

Fig3. Monthly average of sea ice concentration in January of 2014

Estimation of the Arctic sea ice thickness based on the backward tracking analysis

Noriaki Kimura, Hiroyasu Hasumi
Atmosphere and Ocean Research Institute, The University of Tokyo

Since 1972, observations using satellite microwave sensors have provided continuous images of sea ice. It improved our knowledge of sea-ice cover and its temporal and spatial variability. This study aims to derive the ice thickness by a new way based on the backward tracking of sea ice. Thickness is the most important information about sea ice. However, monitoring of the ice thickness is not easy. There have been several attempts to derive the ice thickness from satellite data analysis or numerical models, but these have not yet produced satisfactorily accurate sea ice thickness data. We first analyze the ice trajectory traced back to the ice formation. Based on the derived trajectory, we examine the sea ice age and other parameters such as ice divergence/convergence or heat budget history.

This analysis uses the daily sea-ice velocity derived from satellite microwave sensor AMSR-E and AMSR2 data. The calculation of the ice drifting speed was based on a pattern matching method, the maximum cross correlation technique. This method determined the spatial offset that maximized the cross-correlation coefficient between two brightness temperature arrays in consecutive images separated by 24 hr. After applying filtering and interpolation processes, we constructed a daily ice-velocity dataset without missing data over the sea-ice area on a 60 × 60 km grid for 2003–2022. Backward trajectory is calculated using this daily ice motion. First, particles are arranged at an interval of 10 km over the ice area on a certain day. Daily displacement of particles is calculated from the ice velocity on one-day time steps. When the particle reaches open ocean (no-ice) area, we assume it to be ice production. In this way, birth place, birth day, and trajectory of sea ice were determined. In addition, heat budget was calculated assuming an open water at freezing temperature at the location of the daily particle, and the resulting daily growth was added up to derive the accumulated ice-thickness.

Generally, old thick sea-ice exists the Greenland-Canadian side of the Arctic. The area expands toward the Atlantic side along the north and west coasts of Greenland via the Transpolar Drift Stream and the East Greenland Current, and toward the North American side, moving across the Beaufort Sea to the East Siberian Sea. Sea ice thickness is estimated by developing an empirical formula that relates the sea ice thickness observed in the field to the estimated ice-history parameters such as the accumulated ice-thickness. Comparison of the accumulated ice-thickness with the observed values shows that a constant value multiplied by the accumulated ice-thickness agrees well with the observed ice-thickness. We aim to increase the number of observed values used and derive more versatile formulas for the derivation of the ice thickness by using other ice-history parameters.

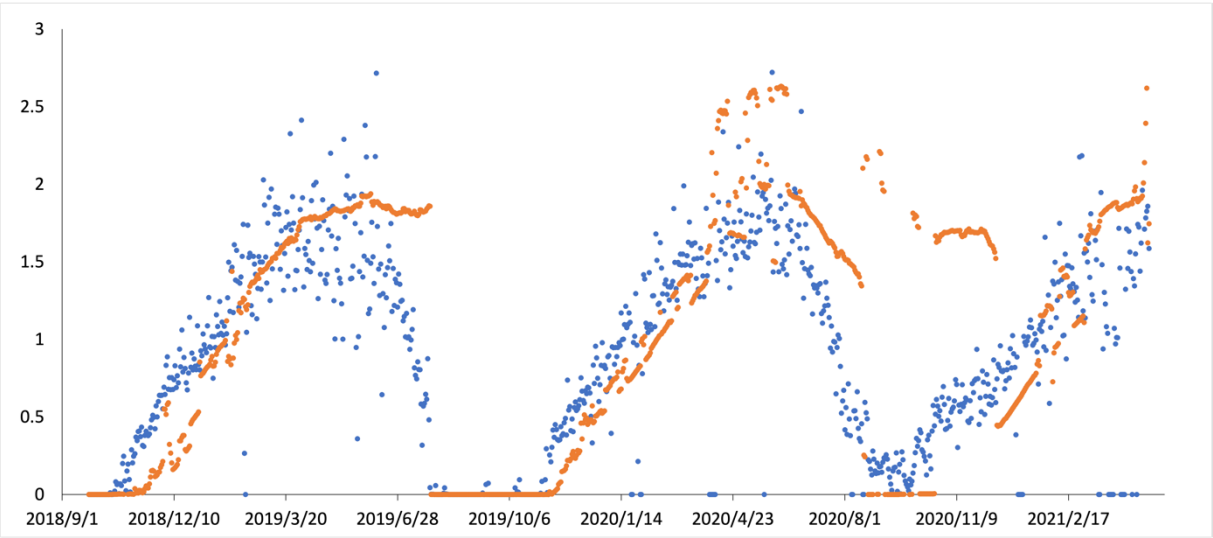

Fig 1. Time-series of the ice thickness observed by moored Upward Looking Sonar (blue dots) and accumulated ice-thickness (orange dots) in the Beaufort Sea

Prediction of summer Arctic sea-ice distribution with a statistical method

Motomu Oyama [1], Hajime Yamaguchi [1] and Noriaki Kimura [2]
[1] *Arctic Sea Ice Information Center, National Institute of Polar Research*
[2] *Atmosphere and Ocean Research Institute, The University of Tokyo*

Arctic Sea Ice Information Center predicts the arctic sea ice distribution from July 1 to September 20 and publishes it on the website in May, June, and July each year. A base of the sea ice forecast method is following Kimura et al (2013). The method assumes that there is a correlation between the sea ice divergence/convergence (SID) from winter to spring and the detrended sea ice concentration (DSIC) in summer. This is because when SID is high, sea ice thickness gets thick and sea ice becomes hard to melt away.

This year, new parameters; sea-ice age (SIA), mean divergence of ice motion (MDI), and an accumulated absolute divergence/convergence of ice motion (AADI) were introduced to that method. These parameters are obtained by backward tracking of sea ice for 4 years (SIA and MDI) or 3 months (AADI). When the particle reaches open ocean area, we assume it to be ice production. In this way, we can determine the SIA. Also, MDI and ADDI are calculated by sea ice divergence and convergence during the life of sea ice. SIA, MDI, and AADI represent the resistance to melting of sea ice related to the ice age or thickness. Ice predictions in the first, second, and third reports are performed by the multiple regression analysis of DSIC, SID, SIA, and MDI, of DSIC, SID, and AADI, and of DSIC, SID, and SIE, respectively.

The predicted ice cover of the September 10 in the first, second, and third reports are shown in Fig 1. There is no significant difference between them on the Russian side, while sea ice distribution on the Beaufort Sea and the Kara Sea is different. The effect of the old ice tongue in the Beaufort Sea is greatest in the third report. The accuracy of these predictions is verified by comparing them with observation, and studies are underway to develop more accurate forecasting methods.

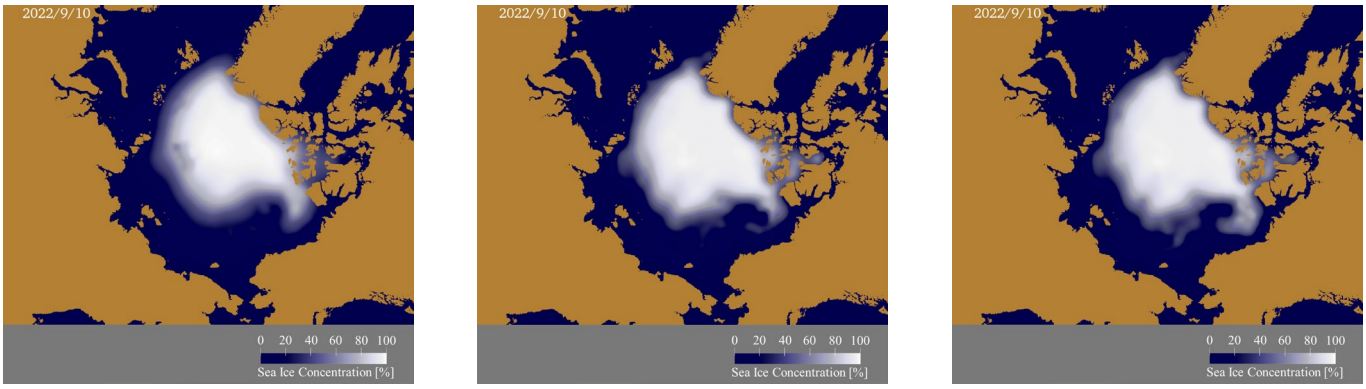

Fig 1: The results of the September 10, 2022 prediction conducted in the first (Left), second (Middle), and third (Right) reports.

References

N. Kimura, A. Nishimura, Y. Tanaka and H. Yamaguchi, Influence of winter sea ice motion on summer ice cover in the Arctic, Polar Research, 32, 20193, 2013.

Modification of Atlantic Water in the Barent Sea

Takao Kawasaki[1], Yoshiki Komuro[2], Jun Ono[2], Hiroyasu Hasumi[1, 2]
[1]*Atmosphere and Ocean Research Institute, the University of Tokyo*
[2]*Institute of Arctic Climate and Environment Research, the Japan Agency for Marine-Earth Science and Technology*

The effects of climate change are particularly apparent as the drastic decline of sea ice in Arctic Ocean (Stroeve and Notz., 2018). Warming of Arctic Ocean has become more pronounced in the recent 20 years (Polyakov et al., 2017). To predict climate change and Arctic sea-ice more than a decade in the future, a climate model that can represent the temperature and salinity of the Arctic Ocean is needed. However, the stratified structure of the Arctic Ocean is not maintained even in the latest climate models, because the mechanism of seawater inflow from other basins has not been sufficiently understood (Ilcak et al., 2016). The water modification in the Barents Sea, where multi-species water inflow and discharge into the Arctic Ocean, is focused on in this study.

A high-resolution (horizontal grid size is 2-8 km in the Barents Sea) ice-ocean model is employed to reproduce the Atlantic water transport and modification in the Barents Sea (Figire 1). The model is driven by 3 hourly sea surface boundary condition of JRA55-do (Tsujino et al., 2018) from 1990 to 2020. Restoring of sea surface salinity is not appled in our simulation.

The temperature, salinity, and mejor pathway of the Atlaintic water are reproduced in our model (Figure 2). The sea ice extent and sea-ice drift velocity are also well calculated. Quantitative analyses of isopycnal and diapycnal transports are conducted. It is found that the sea surface cooling and associated convection induce the loss of buoyancy of seawater in the southern Barents Sea. The vertical mixing with the near surface low-salinity water originated from the melting of sea ice supplies buoyancy to the cooled Atlantic water in the northern Barents Sea.

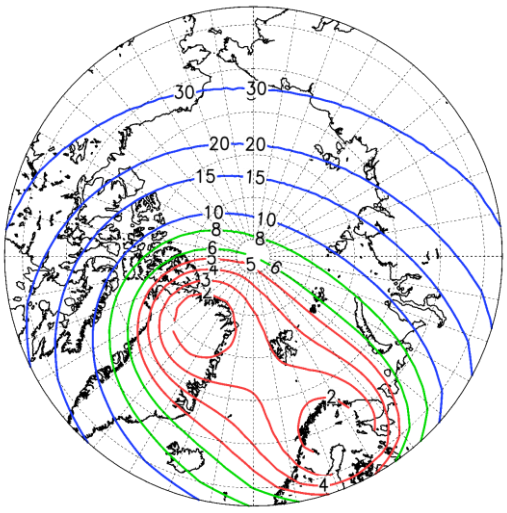

Figure 1: Horizontal grid size in the model.

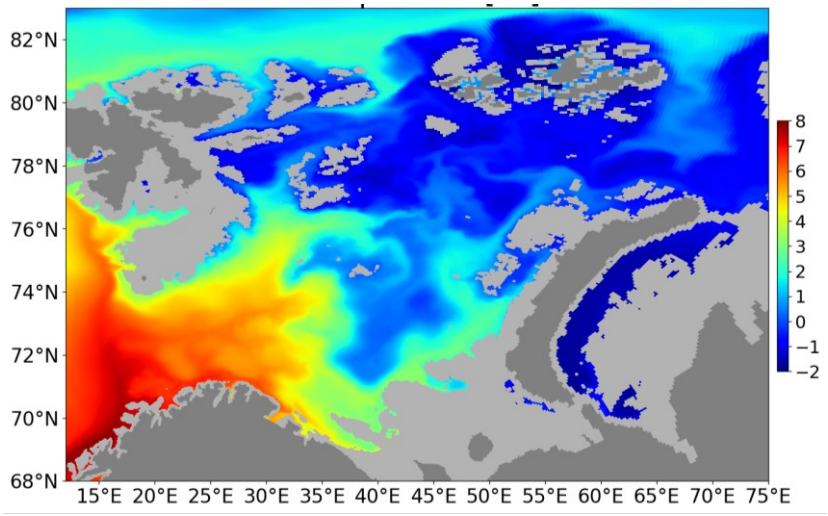

Figure 2: Simulated potential temperature at 150 m depth.

References

Stroeve, J. and D. Notz, Changing state of Arctic sea ice across all seasons, Environmental Resarch Letters, 13, 103001, doi: 10.1088/1748-9326/aade56, 2018

Polyakov, I.V. et.al., Greater role for Atlantic inflows on sea-ice loss in the Eurasian Basin of the Arctic Ocean, Science, 356, 6335, 285-291, doi: 10.1126/science.aai8204, 2017

Ilicak M. et al., An assessment of the Arctic Ocean in a suite of interannual CORE-II simulations. Part III: Hydrography and fluxes, Ocean Modelling, 100, 141-161, doi: 10.1016/j.ocemod.2016.02.004, 2016

Tsujino H. et al., JRA-55 based surface dataset for driving ocean–sea-ice models (JRA55-do), Ocean Modelling, 130, 79-139, doi: 10.1016/j.ocemod.2018.07.002, 2018

Overview of the R/V Mirai Arctic Ocean cruise in 2022

Motoyo Itoh[1], Jonaotaro Onodeara[1], Mariko Hatta[1], Shigeto Nishino[1], Amane Fujiwara[1],
Eiji Watanabe[1], Akihiko Murata[1,2], Takashi Kikuchi[1]
[1]*Institute of Arctic Climate and Environment Research, Japan Agency for Marine-Earth Science and Technology (JAMSTEC)*
[2]*Global Ocean Observation Research Center, Japan Agency for Marine-Earth Science and Technology (JAMSTEC)*

The Arctic Ocean cruise of Research Vessel (R/V) Mirai has been conducted from 12 August to 29 September 2022, under the Arctic Challenge for Sustainability II (ArCS II) project. The Arctic Ocean is the area with the fastest rate of global oceanic warming in the world. The detailed research of the R/V Mirai along with other icebreaking vessels, satellite observation and numerical modeling have documented the impact of inflow of the Pacific origin water. We have observed sea ice decrease and marine ecosystem changes associated with Pacific origin waters bringing heat, nutrients, fresh water into the Arctic. Its impact is getting greater and more wide spread into the entire Arctic.

In 2022, we conducted hydrographic, paleoenvironmental and biogeochemical surveys, including plankton, trace-metals, microplastic, eDNA and aerosols in the Chukchi and Beaufort Seas. Three hydrographic moorings and a sediment trap mooring were also recovered and re-deployed on the pathway of the Pacific origin water to monitor transport and impact on marine ecosystem. In the marginal ice area, various drifting buoys were launched to measure the ocean waves and sea ice interaction. Trials of an under-the-ice drone, designed for automated cruise and observations in the sea ice area, were carried out. In addition to observation of present Arctic environments, sediment records have been collected by piston, gravity, multicore and box corers to understand differences between the present environmental changes and past warming events in the Arctic Ocean.

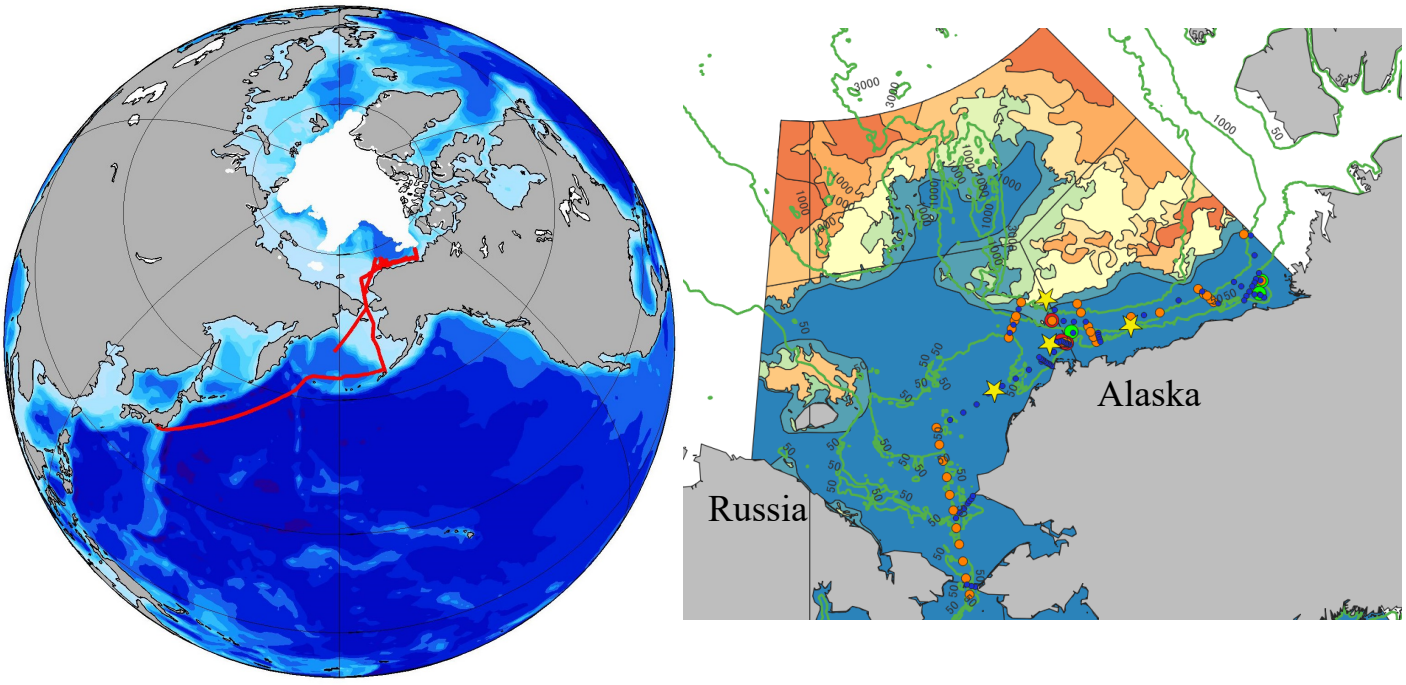

Figure 1. Map of the entire cruise area (left) and enlarged research areas in the Arctic Ocean (right). The cruise track and minimum ice coverate during the observation term from SSM/I (left) and NOAA ice chart (right) are overlayed. Oramge and blue dots shows CTD/R and XCTD stations. Green and red circles denotes moorings and sediment corings stations. Yellow stars shows the locations of under ice drone trials.

Ocean wave observation by multiple drifting buoys in Beaufort Sea of the Arctic Ocean

Tomotaka Katsuno[1], T. Kodara[1], T. Nose[1], R. Uchiyama[1] and T. Waseda[1,2]
[1]*Gladuate School of Frontier Sciences, the University of Tokyo*
[2] *Japan Agency for Marine-Earth Science and Technology (JAMSTEC)*

In the Arctic Ocean, wave phenomena have changed in recent years as a result of the reduction of sea ice. However, there have been few observations of these phenomena. In Arctic open water, the sea ice to its north controls the effective fetch (Thomson and Rogers, 2014). Fetch from the ice edge is difficult to determine due to the high temporal variability in sea ice edge location. The objective of this study was to observe how Arctic Ocean waves grow under off-ice wind conditions where fetch is controlled by the sea ice.
For this purpose, multiple small drifting wave buoys were deployed for direct observation. A total of 15 wave buoys were deployed in the Beaufort Sea in the Arctic Ocean on 2 Sep 2022 during a voyage by the JAMSTEC Research Vessel Mirai (MR22-06C, 11 Aug 2022 ~ 29 Sep 2022) as part of Arctic Challenge for Sustainability II, ArCS II. Two types of buoys were used: 3 SOFAR Spotter buoys (S/N : SPOT-1730, SPOT-1732, SPOT-1803) (https://www.sofarocean.com/products/spotter) and 12 FZ buoys (S/N : FZ02, FZ28~FZ30, FZ33, FZ35~FZ41) produced by our research group. Both buoys use GNSS or Inertial Measurement Units (IMU) to measure the selevation of the sea surface and perform spectral analysis, and transmit the data using Iridium satellites. Some buoys stopped transmitting data by 19 Sep 2022 for several reasons.

The trajectories of the buoys from the time of deployment to 19 Sep 2022 are shown in Figure 1. Also shown is a contour map of sea ice concentration by the AMSR2 satellite on 19 Sep 2022. The buoy was deployed on return from observations in the Marginal Ice Zone (MIZ) during the cruise and was deployed from 71°40'N to 70°20'N around 136°W. The buoy drifted westwards due to the Beaufort Gyre. Each buoy drifted but changed little in relative position.
The significant wave heights and mean periods measured at the buoys during the same period are shown respectively at the top and bottom of Figure 2. The buoys shown above have observed waves with a similar trend for most of the period. However, on 5-6 September 2022, the wave heights and periods were significantly different for each buoy.
The power spectrum density of the buoys around 16:00 (UTC) on 5 Sep 2022, when the difference was the largest, is shown in Figure 3. Together with Fig. 1, it can be seen that buoys located more southerly have observed higher wave heights and longer period waves. This is thought to be due to wave growth caused by winds from the north and requires quantitative analysis. We will furthur investigate the wave growth under off ice wind condition by comparing fetch estimated based on satellite data and also based on fetch laws with the observed buoy data.

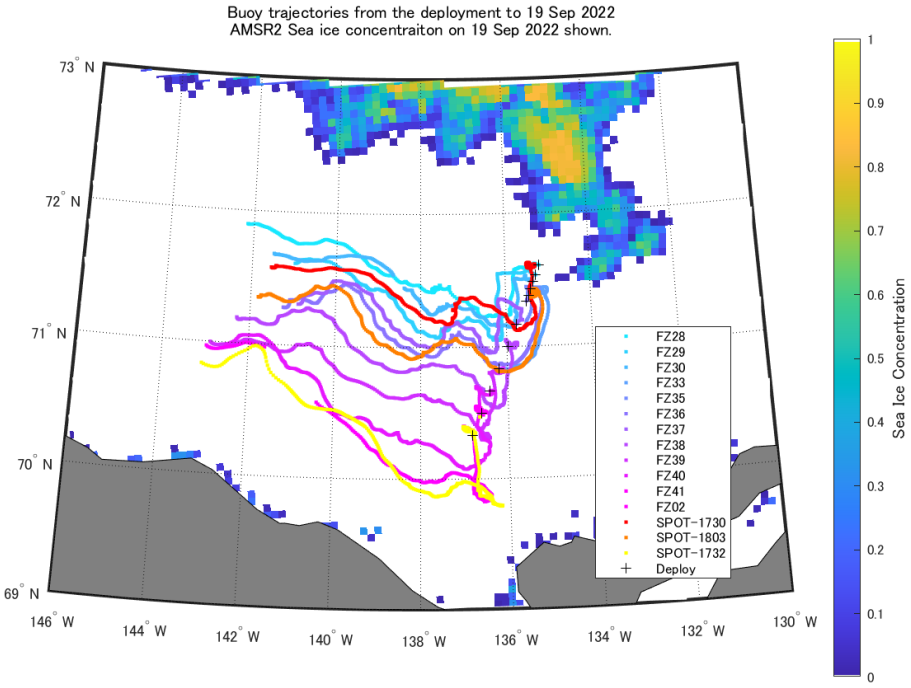

Figure 1. Buoy trajectories from the deployment date (2 Sep 2022) to 19 Sep 2022. The color shows AMSR2 sea ice concentration. Black crosses are the deployment places.

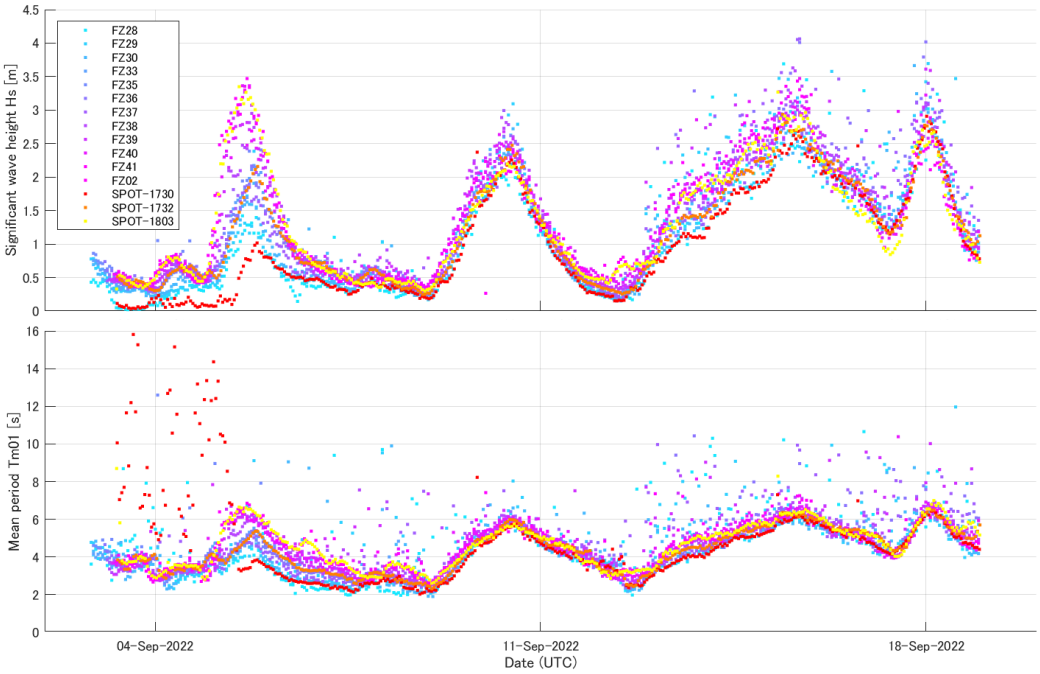

Figure 2. Measured significant wave height (H_s) on the top and mean wave period (T_{m01}) from the deployment date (2 Sep 2022) to 19 Sep 2022.

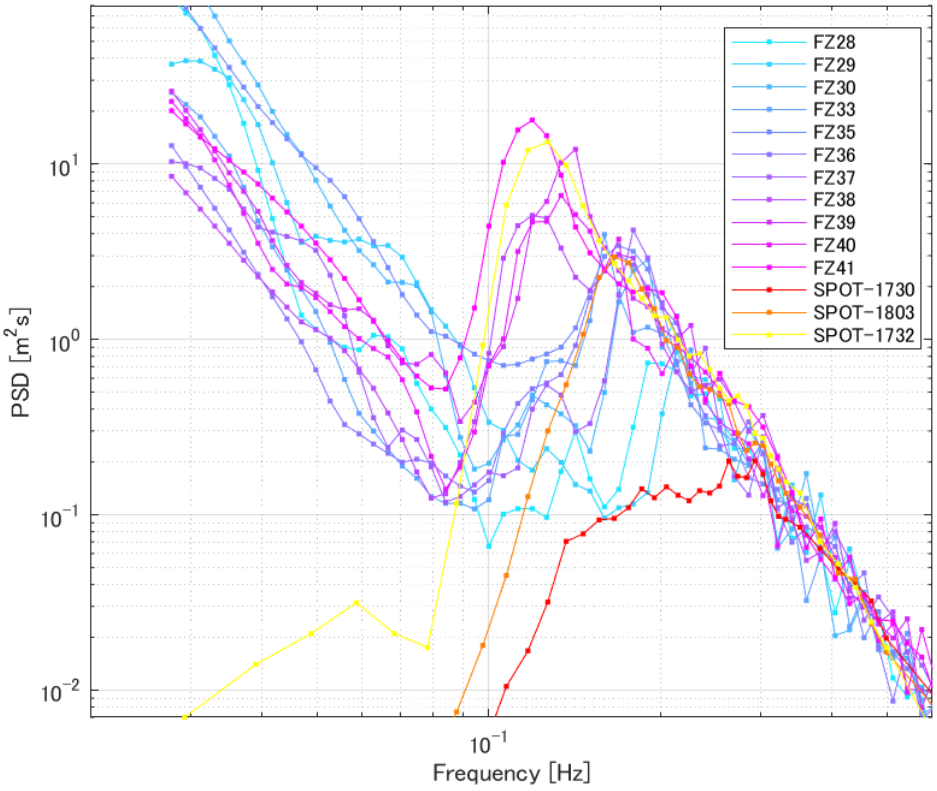

Figure 3. Power spectral density acquired at 15:45~16:15 (UTC) on 6 Sep 2022 for each buoys. For the FZ buoys, the smaller numbered buoys are located further north. For the Spotter buoys, SPOT-1730, SPOT-1803 and SPOT-1732 are deployed from north to south.

References

Thomson J., and W. E. Rogers, Swell and sea in the emerging Arctic Ocean, Geophysics Res. Lett., 41(3136), 2014.

An overview of multi-OpenMetBuoy wave observations in the melting Greenland Sea marginal ice zone

Takehiko Nose[1], M. Hoppmann[2], J. Rabault[3], T. Waseda[1], T. Kodaira[1], T. Katsuno[1], and C. Haas[2]
[1]*GSFS, The University of Tokyo,* [2] *Alfred Wegener Institute,* [3]*The Norwegian Meteorological Institute*

14 OpenMetBuoys (OMB) (Rabault et al. 2022) that measure ocean waves in sea ice were deployed in the Greenland Sea marginal ice zone (MIZ) north west of Svalbard (another buoy, OMB-744, was deployed in the fast ice offshore of east Greenland) during the Polarstern expedition in July--Aug 2022 (PS131). The OMBs were deployed on ice floes of various dimensions ranging from 15 m to as large as ~2km, and thickness, when measured, ranged from 1 m to >2 m. They were spatially distributed to try to cover broad width of the MIZ. The OMBs were deployed opportunistically primarily using the mummy chair (and sometimes using a helicopter) as well as at the three ice camp sites that were revisited three times during PS131. At the ice camp sites, we also deployed Inertial Measurement Unit (IMU) data loggers to capture accelerometer and GNSS time series at roughly 10 Hz frequency. The measurement duration of each OMB varied; the likely reason for instrument ceasing transmissions is that OMB's Iridium communication was affected because the buoy moved sideways (i.e., the antenna is not facing the sky), covered by snow that interfere with radio waves, and/or fell in the ocean as floes melted. Figure 1 shows the OMB trajectories from 12 Jul to 12 Oct 2022.

The primary objective of the PS131 wave buoy deployment was to observe ocean wave effects on the sea ice melt. In this regard, the observation team got the firsthand observational evidence of ice break up due to ocean waves because the ice floe broke into pieces on two occasions during the OMB deployments, of which one was at the ice camp floe that broke into two pieces while they were setting up the camp and deploying instruments. We will introduce the visual footage and wave data for these times in the presentation. There were several other weather events that were captured during the OMB deployments, which we will also introduce.

The power density spectrogram of surface elevation corresponding to the Figure 1 measurement period is provided in Figure 2. The figure shows that various events were captured at different stages of the measurement period. As the ice break up/melts, the floe dimensions were also changing. This is interesting and challenging at the same time; ice floes the buoys were deployed on effectively serve as a floating platform for the wave buoys and their dimensions are changing with time. The scale of ice floes (including horizontal dimension and ice thickness) and incoming wave wavelengths are an important consideration to the wave-ice interaction. So we envisage the dataset (that include ice thickness measurements and TerraSAR match ups) obtained during the PS131 expedition will provide us opportunities to study various aspects of wave-ice interaction including the ocean wave effects on sea ice melt. We will provide overview of the multi-OMB wave deployment data.

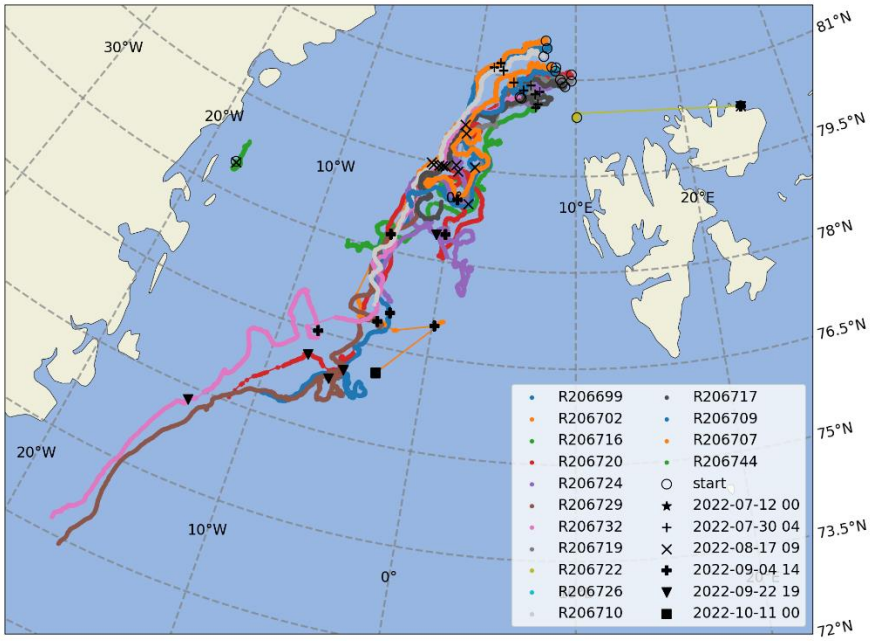

Figure 1. OMB trajectories between 12 Jul and 12 Oct 2022 in the Greenland Sea.

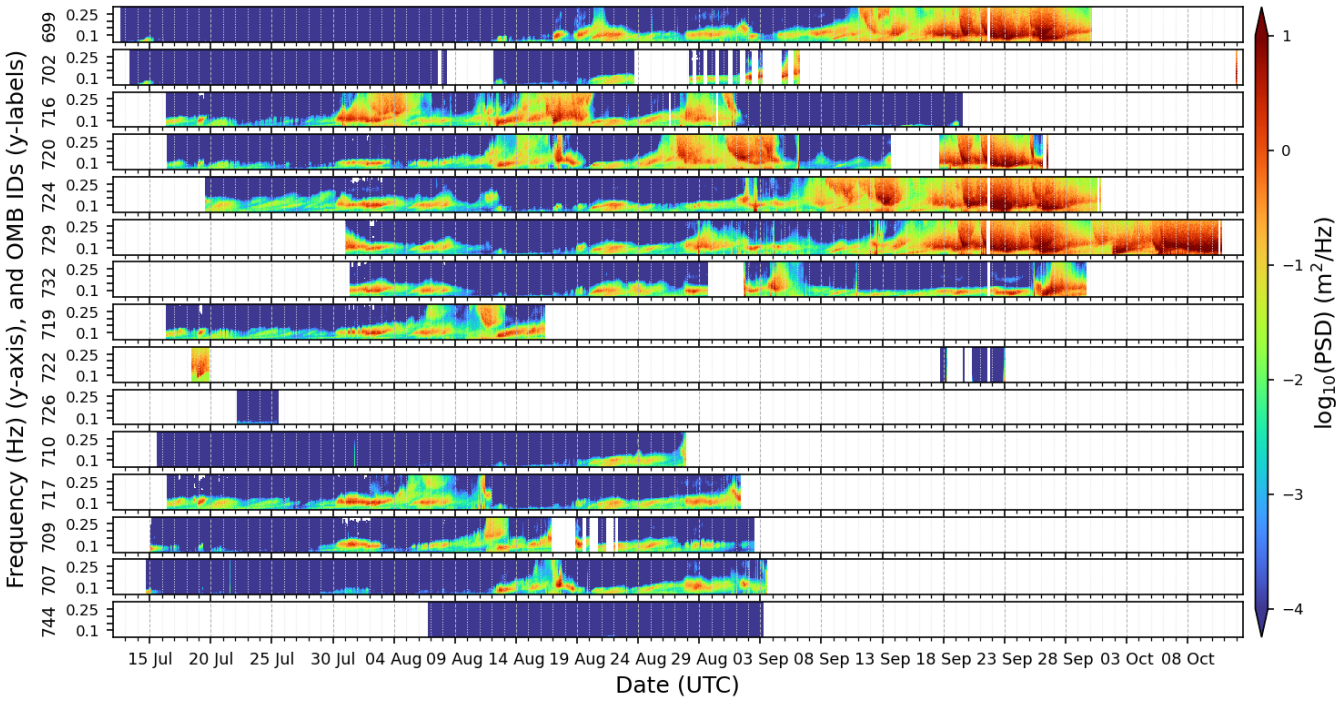

Figure 2. OMB power density spectrogram of surface elevation between 12 Jul and 12 Oct 2022.

Reference

Rabault J., Nose T., Hope G., Müller M., Breivik Ø., Voermans J., Hole L.R., Bohlinger P., Waseda T., Kodaira T., Katsuno T., Johnson M., Sutherland G., Johansson M., Christensen K.H., Garbo A., Jensen A., Gundersen O., Marchenko A., and Babanin A. (2022). OpenMetBuoy-v2021: An Easy-to-Build, Affordable, Customizable, Open-Source Instrument for Oceanographic Measurements of Drift and Waves in Sea Ice and the Open Ocean. Geosciences 12, no. 3: 110. https://doi.org/10.3390/geosciences12030110

Distinct sources of variability in the euphotic depth within the Arctic seas

Taka Hirata[1], Keiko Sato[1], Victor Kuwahara[2], Joji Ishizaka[3], Toru Hirawake[4], Taiga Nakayama[5], Hiroshi Murakami[5]
[1]*Hokkaido University*
[2]*Soka University*
[3]*Nagoya University*
[4]*National Institute of Polar Research*
[5]*Japan Aerospace Exploration Agency (JAXA)*

Growth of phytoplankton in the Arctic seas can be limited by insufficient light necessary for photosynthesis, and understanding the underwater light field plays an essential role in estimating carbon fixation by primary producers in the Arctic seas. However, sufficient in situ ocean observations in the Arctic seas necessary to reveal spatio-temporal variability of the underwater light field are not readily achievable due to its remote geography and harsh environment. As a result, satellite remote sensing is an indispensable technology for investigating the Arctic marine environment, as already proven by sea ice remote sensing. Towards a better understanding of the underwater light field and phytoplankton dynamics in the Arctic seas, the euphotic depth (Z_{eu}), defined as a water depth where Photosynthetically Active Radiation (PAR) at the sea surface attenuates down to its 1% intensity, is investigated using the ocean colour remote sensing data.

Firstly, an ocean colour inversion model was developed based on radiative transfer theory to estimate the euphotic depth. Independent validation of the satellite-derived euphotic depth showed Y = 1.23 X – 6.24 (N=28, r^2=0.68, p<0.01, RMSE=30.11) where Y and X indicate the euphotic depth derived from the satellite and measured in situ, respectively (Figure 1).

Secondly, monthly satellite data of the euphotic depth over the decade of 1998-2007 was analyzed to clarify seasonal and inter-annual variability of the euphotic depth in the Arctic seas. The analysis showed that the euphotic depth was relatively deeper at lower latitudes and shallower in higher latitudes during day-light seasons, being positively correlated with the solar altitude (Figure 2). As a result, it was found that planetary motion was dominating the variability of the euphotic depth in the Arctic seas. However, the euphotic depth in the Russian Arctic seas indicated a stronger influence from another source. The euphotic depth was deeper (shallower) when concentrations of colored dissolved organic matter (CDOM) and suspended hydrosols were lower (higher). As a result, anti-correlations between the euphotic depth and these biogeochemical properties of seawater were found in the Russian Arctic seas, resulting in the reduced positive correlation between the euphotic depth and solar altitude (Figure 2). Indeed, the ocean colour inversion model showed exceptionally high concentrations of CDOM and hydrosols in the Russian Arctic seas. Thus, the variability of the euphotic depth in the Russian Arctic seas was dominated by internal variability of the seawater rather than the planetary motion. Since CDOM reduces the euphotic depth by absorbing solar radiation including PAR, such a high CDOM concentration in the Russian Arctic may indirectly limit primary production, while the exceptionally high CDOM may also contribute to a rise of water temperature that can promote the primary production at the same time. Thus, possible counter-acting effects of CDOM on primary production were implied in the Russian Arctic seas.

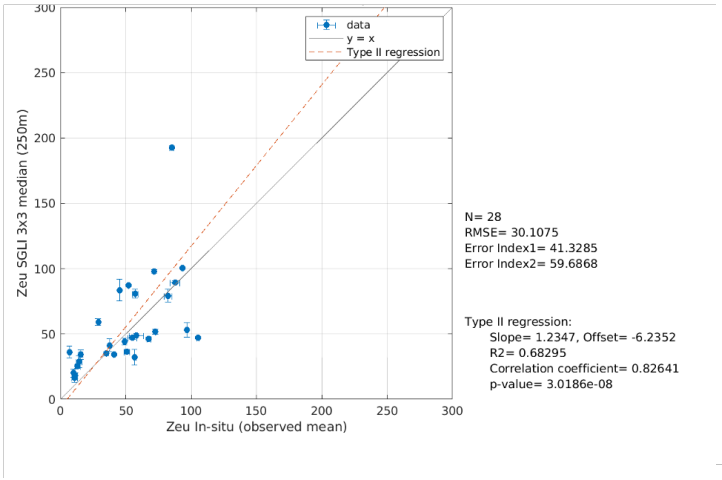

Figure 1. Validation of the satellite-derived euphotic depth.

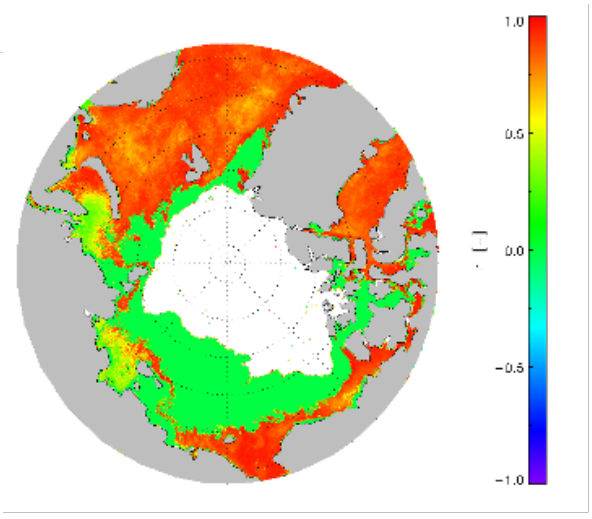

Figure 2. Correlation coefficient between the euphotic depth and solar

Data Manegement of Arctic Project in Japan

Hironori Yabuki[1], Takeshi Sugimura[1] and Takeshi Terui[1]
[1]*Natinal Institute of Polar Research (NIPR)*

Arctic Data archive System (ADS), to promote the mutual use of the data across a multi-disciplinary to collect and share data sets, such as observational data, satellite data, and numerical experiment data. Through these data sets, clarify of actual conditions and processes of climate change on the Arctic region, and further contribute to assessment of the impact of global warming in the Arctic environmental change, to improve the future prediction accuracy.

A new project of the Arctic research (ArCS II :Arctic Challenge for Sustainability II) has been started in 2020. ArCS II is a national flagship project funded by the Ministry of Education, Culture, Sports, Science and Technology(MEXT). The National Institute of Polar Research (NIPR), Japan Agency for Marine-Earth Science and Technology (JAMSTEC) and Hokkaido University are playing the key roles in this project, and will continue to carry it out for approximately four-and-a-half years from June 2020 to March 2025. Arctic Data archive System (ADS) is responsible for the data management of this project.

ADS has granted data DOIs as a system that provides a permanent link to publicly available data.

On the other hand, the Institute of Polar Research publishes a data journal, the Polar Data Journal, for the purpose of distributing quality-controlled real data.

The ADS serves as the primary data repository for the Polar Data Journal. PDJ and ADS contribute to the evaluation of scientific data as scientific assets and research achievements in the ArCS II project..

Figure 1. Top page of ADS

Relationship between Anthropogenic Aerosol Increase and Arctic Surface Cooling in mid-20th Century

Takuro Aizawa[1,2], Naga Oshima[2] and Seiji Yukimoto[2]

[1]*National Institute of Polar Research , Tachikawa, Japan*

[2]*Meteorological Research Institute, Tsukuba, Japan*

Observational records show Arctic surface cooling of −0.95°C–−0.70°C during the mid-20th century (1940–1970) followed by ongoing rapid warming since 1970 (Figure.1). Long-term global warming has been extensively researched and has been primarily ascribed to anthropogenic greenhouse gas forcing. However, the factors contributing to the mid-20th century Arctic surface cooling remain poorly constrained. We conducted the multimodel analyses using the state-of-the-art climate models and quantified contributions to the Arctic surface cooling from greenhouse gases, aerosols, natural forcings, and multidecadal internal variabilities.

Multimodel ensemble mean using all historical simulations in 35 Coupled Model Intercomparison Project Phase 6 (CMIP6) models exhibited weak Arctic surface cooling in 1940–1970, which could be attributed to external forcings. Multimodel ensemble means of using all historical simulation in 13 CMIP6 Detection and Attribution Model Intercomparison Project (DAMIP) models exhibited Arctic surface cooling of −0.22°C (±0.24°C) in decadal mean temperature in 1970 versus that in 1940 and showed that anthropogenic aerosol forcings contributed to a cooling of −0.65°C (±0.37°C), which was partially offset by a warming of 0.44°C (±0.22°C) due to well-mixed greenhouse gases (Figure. 2). The range of the multidecadal internal variability (−0.47°C–0.47°C) is similar to the range of −0.42°C to 0.33°C reported by England et al. (2021). When the multidecadal internal variability was combined with the cooling response to all forcings, its value reached −0.69°C (−0.93°C–−0.45°C), which is comparable to the observed cooling of −0.81°C (Figure. 2). The ranges of 30-year Arctic SAT trends for weak and strong cooling fluctuations caused by the internal variability were estimated to be −0.6°C and −1.2°C with reemergence periods of approximately 70 and 2000 years, respectively. The ongoing warming signal will override the fluctuations due to internal variabilities in the Arctic (Figure. 1). As anthropogenic sulfur emissions and sulfate aerosols contributing to cooling at Earth's surface will decrease in any future scenarios of shared socioeconomic pathways (SSP) (Gidden et al., 2019), Arctic warming will continue over the near-term future even under strong cooling fluctuations generated by internal variability.

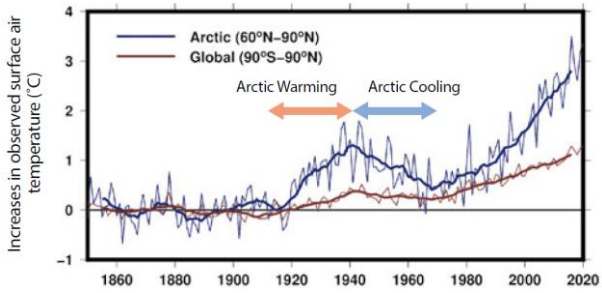

Figure 1. Observed surface air temperature changes in the Arctic (blue line) and Global (red line) relative to the 1850-1900 mean by HadCRUT5. Thick lines indicate 9-year running mean values.

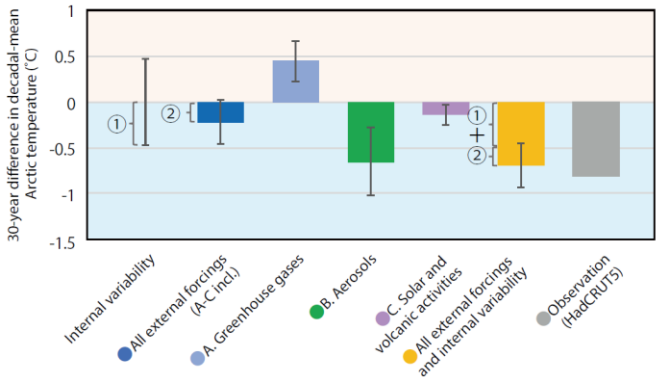

Figure 2. Thirty-year changes (the values in 1970 minus the values in 1940) in the decadal-mean Arctic-averaged SAT due to each external factor, as estimated by multiple climate model analysis. Decadal mean values in 1970 and 1940 are calculated averaging over 1965-1974 and 1935-1944, respectively. Reference: modified from Aizawa et al. (2022) Figure 4.

References

Aizawa, T., N. Oshima, and S. Yukimoto, Contributions of anthropogenic aerosol forcing and multidecadal internal variability to mid-20th century Arctic cooling—CMIP6/DAMIP multimodel analysis, Geophysical Research Letters, 49, e2021GL097093, 2022.

England, M. R., I. Eisenman, N. J. Lutsko, and T. J. W. Wagner, The recent emergence of Arctic Amplification, Geophysical Research Letters, 48, e2021GL094086, 2021.

Gidden, M., K. Riahi, S. Smith, S. Fujimori, G. Luderer, E. Kriegler et al., Global emissions pathways under different socioeconomic scenarios for use in CMIP6: A dataset of harmonized emissions trajectories through the end of the century, Geoscientific Model Development, 12(4), 1443–1475. 2019

Surface melt at SIGMA-B site in Qaanaaq Ice Cap, northwestern Greenland triggered by radiant fluxes in the 2015, 2019, 2020 summers

Motoshi Nishimura[1], Teruo Aoki[1], Masashi Niwano[2], Sumito Matoba[3], Tomonori Tanikawa[2], Satoru Yamaguchi[4], and Tetsuhide Yamazaki[5]

[1]*Arctic Environmental Research Center, National Institute of Polar Research*

[2] *Meteorological Research Institute, Japan Meteorological Agency*

[3] *Institute of Low Temperature Science, Hokkaido University*

[4] *National Research Institute for Earth Science and Disaster Resilience*

[5] *Avangnaq Arctic Project*

An Automatic Weather Station (AWS) was installed at an elevation of 944 m above sea level (SIGMA-B site) on the Qaanaaq ice cap in northwestern Greenland, where continuous weather observations have been conducted since July 2012 (Aoki et al. 2014). The AWS site was estimated to have been near the equilibrium line from 2012 to 2016 based on the results of fixed-point stake observations at different elevations at the Qaanaaq ice cap (Tsutaki et al., 2017). However, amounts of accumulation and ablation at this site and their temporal variation have not been quantified. The mass loss in the low-elevation coastal ice cap is significantly higher than that in the inland ice cap due to the recent temperature rising (Noël et al., 2017), and it is therefore important to quantitatively verify a temporal variation of the surface mass balance at this site.

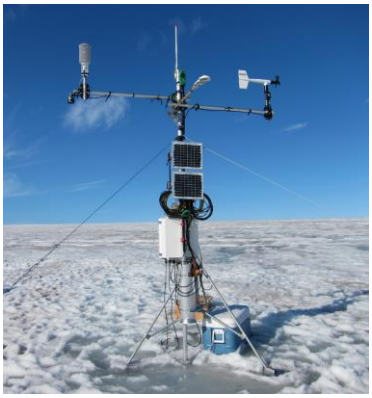

Figure 1. Overview of the AWS system and the ambient environment at SIGMA-B site.

In this study, we investigated the interannual variation of surface energy balance and surface melting rate at the SIGMA-B site to understand the present condition of the snow/ice surface and its accumulation/ablation process based on the ground meteorological observation data obtained over several years at the site.

We used hourly observation data of air temperature, relative humidity, wind direction, wind speed, atmospheric pressure, upward/downward shortwave, and longwave radiations, and snow depth observed by AWS at the SIGMA-B site (77.518° N, 69.062° W) on the Qaanaaq ice cap located in northwest Greenland (Fig. 1). Data from July 2012 to August 2020 were used for the analysis in this study.

The surface energy balance was calculated to estimate surface melt rate using Eqs. (1)–(4). This energy balance analysis included five energy components: net (downward−upward) shortwave radiation (SW_{net}), net longwave radiation (LW_{net}), sensible heat flux (H), latent heat flux (ιE), and sensible heat flux by rainfall (Q_{R}) (Eq. (1); Nishimura et al., 2021). The surface energy balance (SEB) is a variable corresponding to the residual of each energy quantity and is equal to the melt energy when the snow surface temperature is 0 °C and SEB > 0. H and ιE were calculated using the bulk aerodynamic method (Eqs. (2) and (3)). Q_{R} is calculated by Eq. (4). The precipitation data were obtained from the ECMWF ERA-5 data with every 0.25° spatial resolution (Hersbach, 2018). This study used an index of cloudiness (N_ε) (Eq. (5)) calculated using surface air temperature, relative humidity, and downward longwave radiation (Konzelmann et al., 1994; van den Broeke et al., 2004; Conway et al., 2015). The index was defined between 0 (clear-sky condition) and 1 (overcast condition). This study defined the direction of energy transport to the snow/ice surface as positive.

$$SEB = SW_{\mathrm{net}} + LW_{\mathrm{net}} + H + \iota E + Q_{\mathrm{R}}, \quad (1)$$

$$H = \rho\, C_{\mathrm{p}}\, C_{\mathrm{H}}\, U\, (T_{\mathrm{a}} - T_{\mathrm{s}}), \quad (2)$$

$$\iota E = \rho\, \iota\, C_{\mathrm{E}}\, U\, (q_{\mathrm{a}} - q_{\mathrm{s}}), \quad (3)$$

$$Q_{\mathrm{R}} = P_{\mathrm{r}}\, \rho_{\mathrm{w}}\, l_{\mathrm{w}}\, (T_{\mathrm{w}} - T_{\mathrm{s}}), \quad (4)$$

$$N_\varepsilon = (\varepsilon_{eff} - \varepsilon_{cs})/(\varepsilon_{ov} - \varepsilon_{cs}). \quad (5)$$

Radiant flux absorbed by the snow surface (R) is also defined as a total of SW_{net} and downward longwave radiation absorbed by snow ($\varepsilon LW_{\mathrm{d}}$), where ε (= 0.98; Armstrong and Brun, 2008) is the snow/ice surface emissivity. Since R is a major source of energy input, the temporal variation of it is a vital component to consider the surface energy balance.

In 2014/15, 2018/19, and 2019/20, the amount of surface melting was large (2014/15: 923, 2018/19: 976, 2019/20; 888 [mm w.e.]); the amount of melting was more than 1.4 times higher than the observation period average. In these years, higher

temperatures and lower albedo were observed. Those years were the three largest SW_{net} years during the observation period. This result suggests that the albedo feedback may have increased SW_{net} and triggered the surface melting.

The mean SW_{net}, εLW_d, and R in every year's summer and those variations are shown in Table 1 and Fig. 2. The year with the largest summer mean SW_{net} was 2019/20 (85.4 W m^{-2}), followed by 2014/15 (84.3 W m^{-2}). On the other hand, the year with the largest summer means εLW_d and R were 2018/19 (εLW_d: 271.4, R: 347.1 W m^{-2}). N_ε in the 2014/15 and 2019/20 summers were low, implying clear skies condition was dominant and N_ε in the 2018/19 summer was not low (Fig. 2b). Because downward longwave radiation increases under overcast conditions due to the additional black body radiation from cloud-cover, the snow surface was also possibly heated by a large amount of R with relatively more cloudy condition continued in the 2018/19 summer than in other two summers. Considering the largest surface melting occurred in the 2018/19 summer, not only the contribution of shortwave radiation from clear skies but also that of longwave radiation is important for the surface melting

Table 1. Mean summer (June, July, and August) radiant fluxes (SW_{net}, εLW_d, and R) in each year. Those ensemble averages and standard deviations are also listed in the bottom.

Year (JJA)	SW_{net} W m^{-2}	εLW_d W m^{-2}	R W m^{-2}
2011/12	64.7	267.5	349.0
2012/13	52.9	265.4	317.1
2013/14	56.8	273.4	330.0
2014/15	**84.3**	**252.8**	**336.0**
2015/16	66.3	268.2	335.0
2016/17	59.8	262.9	323.6
2017/18	53.4	265.9	319.6
2018/19	**74.4**	**271.4**	**347.1**
2019/20	**85.4**	**255.1**	**339.3**
average	66.4	264.7	333.0
SD	11.7	6.5	10.7

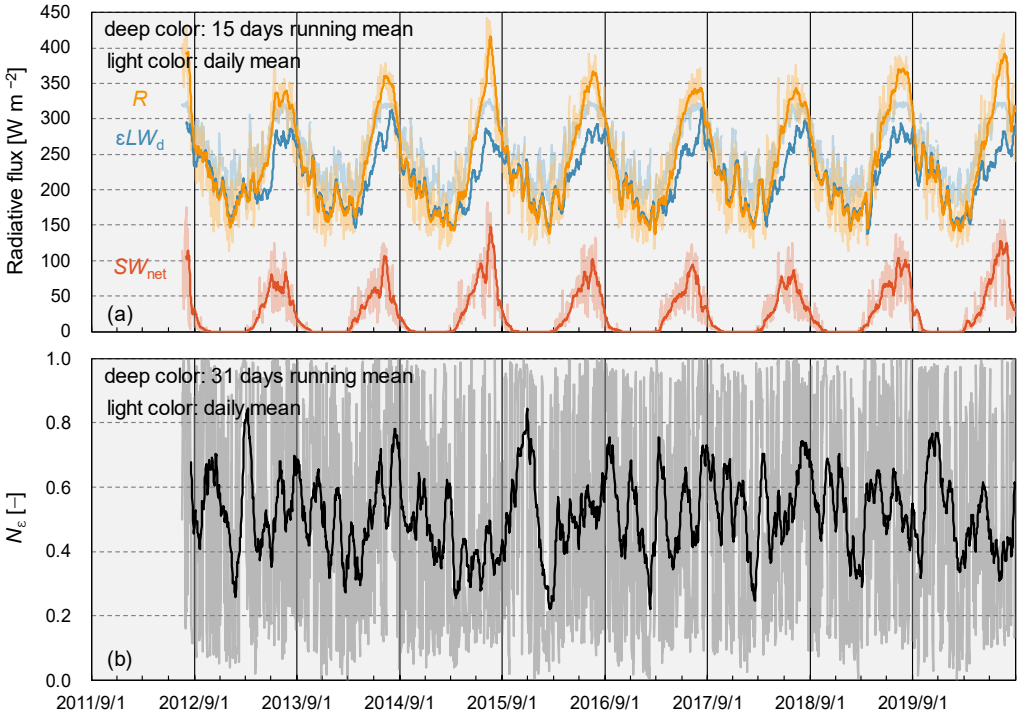

Figure 2. (a) Variation of daily mean net shortwave radiation (SW_{net}), downward longwave radiation (LW_d), and their combined input total radiation ($R^{\downarrow}$). (b) Variation of daily mean cloud cover index.

References

Aoki, T. et al., Bull. Glaciol. Res., 32, 3–20. https://doi.org/10.5331/bgr.32.3, 2014.

Armstrong, R. L. and Brun, E. (Eds.).: Physical processes within the snow cover and their parameterization, Snow and Climate: Physical Processes, Surface Energy Exchange and Modeling, Cambridge University Press, Cambridge N.Y., p. 58, 2008.

Conway, J. P. and Cullen, N. J., Int. J. Climatol., 35, 699–713. https://doi.org/10.1002/joc.4014, 2015.

Hersbach, H. et al., ERA5 hourly data on single levels from 1959 to present. Copernicus Climate Change Service (C3S) Climate Data Store (CDS). (Accessed on September 12, 2022), 10.24381/cds.adbb2d47, 2018.

Konzelmann, T. et al., Global Planet. Change, 9, 143–164. https://doi.org/10.1016/0921-8181(94)90013-2, 1994.

Nishimura, M. et al., Environ. Res. Comm., 3(051003), 1–16. https://doi.org/10.1088/2515-7620/abfcae, 2021.

Noël, B. et al., Nat. Comm., 8(14730). https://doi.org/10.1038/ncomms14730, 2017.

Tsutaki, S. et al., Ann. Glaciol., 58, 181–192. https://doi.org/10.1017/aog.2017.7, 2017.

van den Broeke M. R. et al., Journal of. Atmospheric. Oceanic Technology. 21: 1417–1431, https://doi.org/10.1175/1520-0426(2004)021<1417:AAITQO>2.0.CO;2., 2004.

Mass loss of Qaanaaq Ice Cap in northwestern Greenland from 2012 to 2022

Kaho Watanabe[1,2], Ken Kondo[1,2] and Shin Sugiyama[1]
[1] *Institute of Low Temperature Science, Hokkaido University*
[2] *Graduate School of Environmental Science, Hokkaido University*

Peripheral glaciers and ice caps in Greenland account for 13 % of the global glacier mass loss from 2000 to 2019 (IPCC, 2021). Despite observations showing recent increase in ice loss in northwestern Greenland (Kjær et al., 2012), details of the spatial and temporal variabilities of the glacier change remain unclear because only a few in-situ glaciological studies have been reported in northern Greenland. To acquire a long-term glacier mass balance and better understand the mechanisms of its temporal variations, we have conducted surface mass balance and surface elevation measurements on Qaanaaq Glacier, an outlet glacier of Qaanaaq Ice Cap in northwestern Greenland since 2012 (Figure 1) (Sugiyama et al., 2014). In this study, we quantified the mass change of Qaanaaq Ice Cap from 2012 to 2022 and compared the result with meteorological data collected on the ice cap at 944 m a.s.l. (SIGMA-B) (Aoki et al., 2014). We also compare the surface mass balance with elevation change to study the role of the ice dynamics in the observed glacier thinning.

Surface mass balance was measured by using aluminum poles installed at six locations distributed at 243–968 m a.s.l. (Figure 1b). The height of the poles above the ice or snow surfaces was measured every August to obtain annual specific balance at each site. Snow density was measured when the glacier surface was covered with snow to calculate water equivalent snow depth. Mean specific mass balance over the entire ice cap was computed for each year, by assuming that surface mass balance is a function of elevation. Glacier surface elevation was measured by kinematic GPS surveys in July–August 2012, 2019 and 2022. The survey was performed along the central glacier flowline with approximate intervals of 22 m.

The results of the mass balance measurement from 2012 to 2022 showed 10-year-mean specific balance of 0.15 m w.e. a^{-1} at 968 m a.s.l. and −1.67 m w.e. a^{-1} at 243 m a.s.l.. Significant interannual variations of ~2 m w.e. a^{-1} were observed at each site. The cumulative mass balance of the ice cap from 2012 to 2022 was −4.02 ± 0.22 m w.e.. The most negative specific mass balance was observed in 2014/15 (−1.08 ± 0.04 m w.e. a^{-1}), which we attribute to relatively high summer temperature (degree day factor of 208 ℃ d and small amount of snow accumulation (0.27 ± 0.11 m w.e. a^{-1}). The glacier surface elevation dropped from 2012 to 2022, with a rate greater in 2019–2022 (−0.87 m a^{-1}) than in the earlier period of 2012–2019 (−0.61 m a^{-1}). The magnitude of the rate increased in the later period particularly in the middle of the ablation zone, whereas the change was smaller in the regions near the equilibrium altitude and near the terminus. Comparison of the elevation change and surface mass balance suggested that ice thickness change was affected by slowdown of the glacier. We attribute the recent acceleration in the ice loss to more negative surface mass balance and changes in the glacier flow speed.

Our results imply that glaciers and ice caps in the Qaanaaq region are rapidly losing mass over the last decade at a rate varying from year to year. Warming climate is the most important driver of the mass loss, but changes in the snow accumulation play a key role as well. Continuous effort for monitoring glacier mass balance and ice dynamics is required for furthering our understanding of the mass loss of glaciers in Greenland and the Arctic.

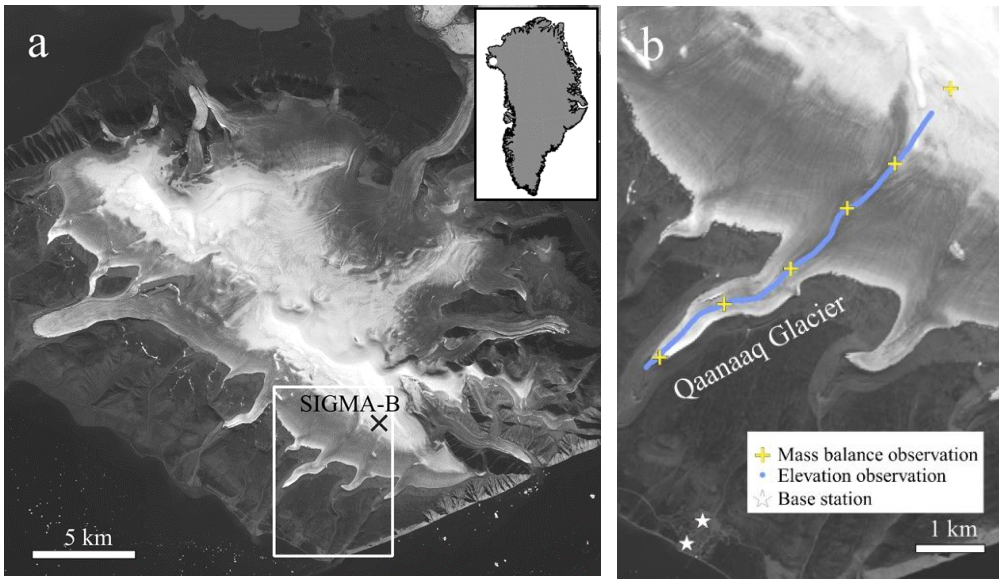

Figure 1. (a) Satellite image (Landsat 8, 25 July 2020) showing Qaanaaq Ice Cap, northwestern Greenland. The box indicates the area shown in (b). The location of the weather station (SIGMA-B) is indicated by ×. (b) Satellite image of Qaanaaq Glacier. The mass balance observation sites are indicated by ＋, and the surface elevation was measured along the blue line. The base stations of the GPS survey were installed at the locations indicated by ★.

References

Aoki et al., Field activities of the “snow impurity and glacial microbe effects on abrupt warming in the Arctic” (SIGMA) project in Greenland in 2011–2013, Bulletin of Glaciological Research, 32, 3–20, 2014.

IPCC, Climate Change 2021: The Physical Science Basis. Contribution of Working Group I to the Sixth Assessment Report of the Intergovernmental Panel on Climate Change, Cambridge University Press, In Press, 2021.

Kjær et al., Aerial photographs reveal late-20th-century dynamic ice loss in northwestern Greenland, Science, 337 (6094), 569–573, 2012

Sugiyama et al., Initial field observation on Qaanaaq ice cap, northwestern Greenland, Annals of Glaciology, 55(66), 25–33, 2014.

Ground penetrating radar survey on Qaanaaq Glacier in northwestern Greenland

Ken Sato[1], Shin Sugiyama[2]
[1] *Graduate school of Environmental Science, Hokkaido University*
[2] *Institute of Low Temperature Science, Hokkaido University*

To study changes in peripheral glaciers and ice caps in Greenland, we have been running field observations on Qaanaaq Ice Cap in northwestern Greenland (77º28' N, 69º14' W) under the projects of GRENE (2012–2016), ArCS (2016–2020) and ArCS II (2020–). Qaanaaq Ice Cap has an area of 289 km^2 with an elevation range of 30–1110 m. In the summer 2022, we performed a GPR (ground penetrating radar) survey on Qaanaaq Glacier (Figure 1), an outlet glacier of the ice cap. The GPR measurement was performed from 18th July to 12th August 2022, using a GPR system (SIR-4000, 3200 MFL) manufactured by GSSI, Inc. The system consists of a controller, transmitter, receiver and 2.4 m long antennae. The central frequency of the radar wave was 40 MHz. During the survey, reflection waves received within a time range of up to 2700 ns were recorded, which is equivalent to the ice depth up to 226 m. The measurement was performed along 14 survey routes, i.e. seven sections perpendicular to the ice flow direction, one long section along six mass balance stakes, and four additional sections along the side margins of the glacier (Figure 1). The total length of the survey routes was 21.13 km.

The reflection image obtained along the uppermost transverse section (Figure 1, section 1) is shown in Figure 2. Two-way travel time was converted to ice thickness by assuming a wave propagation velocity of 168 m s^{-1} in the glacier. The maximum depth along the section 1 was approximately 160 m. A clear v-shaped depression was observed on the bed at 1000 m from the eastern margin of the survey section (Figure 2). Results obtained at other transverse sections indicated that this depression continues downstream. In addition to reflections from the bed, strong reflections were recorded within the glacier from the surface to the bed at about 800 m from the eastern margin of the survey section (Figure 2). Based on our in-situ observation on the glacier, we attribute these englacial reflections to meltwater in a crevasse.

The GPR data provided information on ice thickness, bed geometry and englacial structures, which are crucial to study physical processes of the glacier as well as to quantify the volume of ice. Most importantly, these data help us to understand the englacial and basal hydrology in polythermal glaciers in the Arctic.

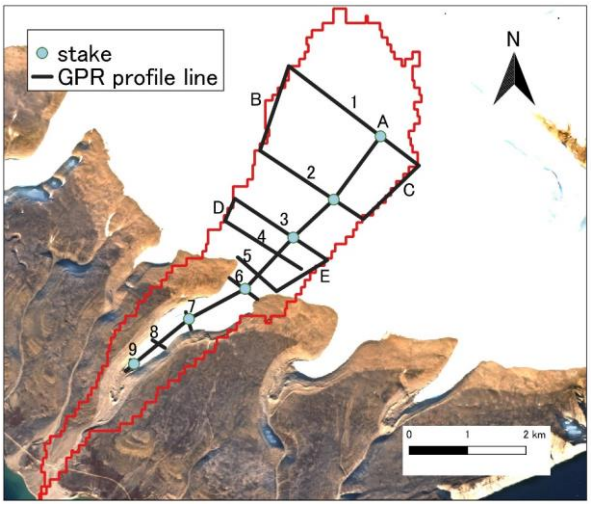

Figure 1. GPR survey routes and mass balance stake locations on Qaanaaq Glacier.
The background is a satellite image acquired on Sep. 17, 2022

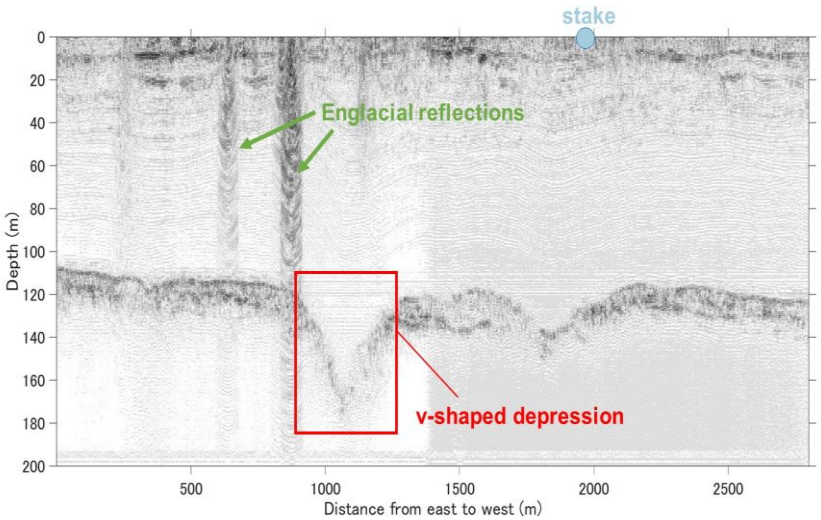

Figure 2. GPR profile along the section 1 in Figure 1.
Horizontal axis shows the distance from the eastern margin of the survey route.

References

Sugiyama, S., Sakakibara, D., Matsuno, S., Yamaguchi, S., Matoba, S. and Aoki, T., 2014. Initial field observations on Qaanaaq ice cap, northwestern Greenland, Annals of Glaciology, 55(66), 25-33.

Meltwater discharge from Qaanaaq Glacier in the summer 2022

Takuro Imazu[1,2], Ken Kondo[1,2] and Shin Sugiyama[1]
[1]*Institute of Low Temperature Science, Hokkaido University*
[2]*Graduate school of Environment Science, Hokkaido University*

Under the influence of air temperature rise in the Arctic, glacial meltwater discharge has been increasing in Greenland (e.g., Bamber et al., 2012). Unprecedented amount of discharge caused flooding, which resulted in damages of infrastructures in the coastal settlements in Greenland (Mikkelsen et al., 2012). For example, floods occurred in 2015 and 2016 at an outlet stream of Qaanaaq Glacier in northwestern Greenland destroyed a bridge and a road (Kondo et al., 2021). After the flood events, we began measurements of the stream discharge to investigate a link between recent climate change and the flooding. Based on the measurements from 2017 to 2019, we constructed a glacier runoff model and demonstrated that the floods were caused by intensive melt of the glacier in 2015, whereas by a heavy rain event in 2016. In the summer 2022, the discharge from Qaanaaq Glacier flooded again on 17 July and damaged the road connecting Qaanaaq Airport and the settlement of Qaanaaq (Fig. 1). This event highlights the need for further research in the region. To investigate the processes controlling the river discharge variations, we performed discharge and glacier melt measurements in the summer 2022.

Discharge from Qaanaaq Glacier was measured at 2.0 km from the glacier from 20 July to 26 August (Fig. 2). Water level of the stream was obtained every 10 minutes with a pressure sensor (HOBO U20-001-04) fixed within the water in the stream. Water current was measured 31 times every 0.5 m across the stream with an electromagnetic current meter (YOKOGAWA ES-7603) to compute the discharge by integrating the current over the cross-sectional area. The discharge measurements were repeated 31 times during the study period, so that observed water level variations were converted to discharge time series by using an empirical relationship between water level and discharge. Meteorological data was obtained from Qaanaaq Airport located at 16 m a.s.l. (Fig. 2). During the observation period, the discharge varied within a range from 0.21 to 2.72 $m^3 s^{-1}$ (Fig. 3). The lowest discharge was observed on 22 August when daily air temperature dropped to 3.9 °C (Fig. 3). On 17 July, the day of the flood event, air temperature increased to 11 ℃. This is the highest temperature during the summer 2022, suggesting the flood event was likely due to intensive glacier melt. Glacier runoff modelling is planned to investigate the processes drove the flood in 2022.

Figure 1. The food event on 17 July 2022.
The photograph was taken at the discharge measurement site indicated in Fig. 2.

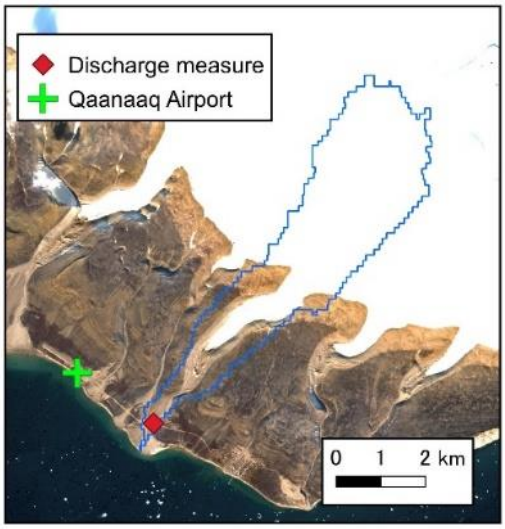

Figure 2. Sentinel-2 image of the study site (9 September 2022), showing the locations of the discharge measurement site(＋) and a weather station at Qaanaaq Airport (♦)

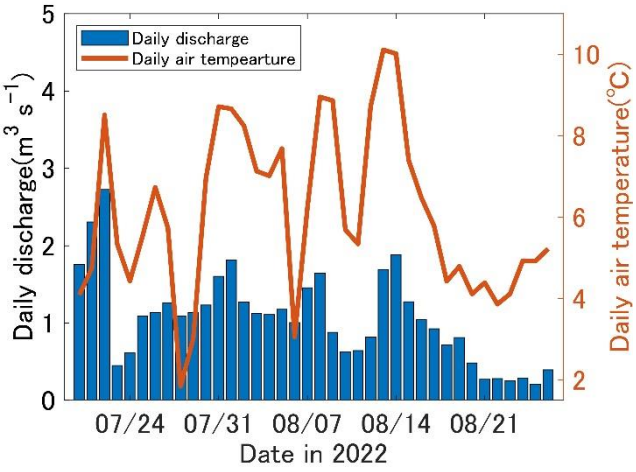

Figure 3. Daily discharge of the outlet stream of Qaanaaq Glacier (left) and daily mean temperature measured at Qaanaaq Airport (right) from 20 July to 26 August 2022

References

Bamber J, van den Broeke M, Ettema J, Lenaerts J and Rignot E, Recent large increases in freshwater fluxes from Greenland into the North Atlantic, Geophysical Research Letters 39(19), L19501, 2012.

Mikkelsen AB and 9 others, Extraordinary runoff from the Greenland Ice sheet in 2012 amplified by hypsometry and depleted firn-retention, The Cryosphere 10(3), 1147–1159, 2016.

Kondo K, Sugiyama S, Sakakibara D, Fukumoto S, Flood events caused by discharge from Qaanaaq Glacier, northwestern Greenland, Journal of Glaciology 67(263), 500–510, 2021.

Russia's international Arctic policy after the invasion of Ukraine : Experts' voices in the domestic media

Marina Lomaeva, Fujio Ohnishi
Hokkaido University Arctic Research Center

In the second year of Russia's chairmanship of the Arctic Council (AC), the other seven member states unanimously condemned its invasion of Ukraine and suspended cooperation with Russia (the Barents Euro-Arctic Council, the International Arctic Science Committee (IASC) took similar steps etc.) (Bloom, Riedel et al.). This isolation – along with security challenges posed by Finland and Sweden's decision to join NATO – became a major topic in Russia's domestic media, as the Arctic narrative has traditionally been high on the agenda in Putin's Russia (similar to the Soviet period).

This paper reviews the assessments of the current situation and forecasts by Russian experts published in March-October 2022 in the domestic media (the Russian government further tightened its control over them after the invasion), ranging from digital broadsheets (such as *Izvestia*, *Nezavisimaya Gazeta*, and *RIA Novosti*) to local papers (e. g. *Sankt-Peterburgskie Vedomosti*) and portals specializing in the Arctic and international issues (such as *Go Arctic, Arctic : Territory of Dialogue, Russian International Affairs Council (RIAC)'s website* etc.). These experts represent such centers of international relations research in Russia as MGIMO University, Russian Academy of Sciences Institutes (the Institute of World Economy and International Relations (IMEMO), Institute of Northern Europe etc.), Saint-Petersburg State University, and think tanks (the Russian International Affairs Council, Russian Institute for Strategic Studies, Institute of Regional Expertise etc.).

Below is a summary of the main points of these commentaries, columns and interviews.

- Decision on the exclusion of Russia from the AC by the rest of its member states breaches the consensus as a decision-making rule of this forum and undermines the legitimacy of AC (Danyuk cited in Kazargin). The situation is further exacerbated by proposals of new cooperation frameworks excluding Russia such as Nordic Plus or Arctic Council 2.0 (see Kirchner, Rogoff). Such steps may jeopardize the Arctic foothold of such states as Denmark (connected to the Arctic only via Greenland) and the US, which is facing serious competition from China (as demonstrated, for instance, by comparison of the two states' icebreaker fleet) (Belukhin, Fedorov).
- If the current deadlock persists, Russia will have to consider such alternative forums for discussion of the Arctic agenda as the Arctic Circle or Arctic Frontiers (Lipunov, Zhuravel, Korchunov1).
- Scientific research in the Arctic, which is pivotal to studying the impacts of global climate change, requires the participation of Russia as the largest Arctic state (Lipunov, Labetskaya, Mikhailichenko).
- In the face of the boycott by the rest of the AC states, Russia will concentrate its efforts on the domestic Arctic agenda, inviting non-Arctic states such as China or India to join partnerships with Russian public bodies and private companies for the development of the Russian Arctic zone (AZ) (Lipunov, Zhuravel, Arctic : Territory of Dialogue).
- The closure of the Northern Sea Route to the vessels of unfriendly states is the necessary security measure in response to NATO's expansion and its military maneuvers in the Arctic (Fedorov).
- Science diplomacy, in which non-state actors are the key players, may pave the way out of the current deadlock. The expert community should act in the interests of humanity in general (Sergunin, Devyatkin cited in Sukhoverkova).

Most experts concur that international dialogue and cooperation in the Arctic are crucial for the sustainable development of the Russian AZ, although they emphasize Russia's self-sufficiency (Koktysh cited in Kazargin). The gradual worsening of the relations with the rest of the AC members led Russia to reconsider its "exclusionist" stance (formerly shared with Canada) on the non-Arctic states' involvement in the Arctic, although experts show apprehensions about the consequences of the breakup of the AC regional unity and the advance of "extra-regional" players such as China or the UK (Lipunov, Izvestia). Although the mediation by the expert community could be beneficial, considering the impressive record of scientific cooperation in the Arctic since the Murmansk Initiative, it appears problematic in view of the tight control (financial, regulatory) of the federal agencies over research and educational institutions and activities, as well as the media.

References (last accessed on 14.10.2022; in Russian unless otherwise specified)

1. Abdullin, R. “Point of No Return : Will Russia Lose the Arctic?”. *RIA Novosti*. 21.07.2022. Citing Zhuravel, V. (Leading researcher of the Center of Northern Europe, the Institute of Europe of the Russian Academy of Sciences) and Ermakov, S. (Leading expert at the Research Coordination Center, Russian Institute for Strategic Studies). URL: https://ria.ru/20220721/politika-1803829818.html
2. *Arctic : Territory of Dialogue*. “Prospects for International Cooperation in the Arctic Discussed at the Saint-Petersburg International Economic Forum”. 20.06.2022. URL: https://forumarctica.ru/news/na-pmef-otsenili-perspektivy-mezhdunarodnogo-sotrudnichestva-v-arktike-/
3. Belukhin, N. (Junior Research Fellow at IMEMO RAS) “Rebillious Islands : Greenland and the Faroes are Harboring Sovereign Ambitions”. *Russian International Affairs Council: RIAC*. 22.08.2022. URL: https://russiancouncil.ru/analytics-and-comments/columns/arcticpolicy/nepokornye-ostrova-grenlandiya-i-farery-leleyut-suverennye-ambitsii/
4. Bloom, E. T. “A New Course for the Arctic Council in Uncertain Times” [in English]. *Arctic Today*. 18.03.2022. URL: https://www.arctictoday.com/a-new-course-for-the-arctic-council-in-uncertain-times/
5. Fedorov, E. “Ice Curtain : Russia *vs.* NATO in the Arctic”. 30.08.2022. *Military Review*. URL: https://topwar.ru/200838-ledjanoj-zanaves-rossija-protiv-nato-v-arktike.html
6. *Izvestia*. “The US Will Cooperate with Finland and Sweden as Part of the New Arctic Strategy”. 7.10.2022. URL: https://iz.ru/1406970/2022-10-07/ssha-budut-sotrudnichat-s-finliandiei-i-shvetciei-v-ramkakh-novoi-strategii-v-arktike
7. Kazargin, A. “The US is Resuming the Meetings of the Arctic Council without Russia”. *Sankt-Peterburgskie Vedomosti*. 17.06.2022. Citing Koktysh, K. (Associate professor at MGIMO) and Danyuk, N. (Assistant head of the Institute of Strategic Studies and Forecasting (ISIP) at the Russian People’s Friendship University). URL: https://spbvedomosti.ru/news/country_and_world/ssha-vozobnovit-rabotu-arkticheskogo-soveta-bez-uchastiya-rossii/
8. Kirchner, S. “Nordic Plus: International Cooperation in the Arctic enters a New Era” [in English]. *Polar Research and Policy Initiative (PRPI)*. 6.03.2022. URL: https://polarconnection.org/nordic-plus-cooperation-arctic/
9. Korchunov, N. “Russia is interested in the development of mutually beneficial cooperation in the Arctic”. *Arctic : Territory of Dialogue*. 20.07.2022. URL: https://forumarctica.ru/news/rossija-zainteresovana-v-razvitii-vzaimovygodnyh-form-mezhdunarodnogo-sotrudnichestva-v-arktike-/
10. Labetskaya, E. (Lead Researcher at IMEMO RAS). “The Arctic as a Battleground : Russia’s Leadership Under Threat”. *Nezavisimaya Gazeta*. 29.05.2022. URL: https://www.ng.ru/dipkurer/2022-05-29/9_8447_arctic.html
11. Lipunov, N. (Analyst at the Institute for International Studies, MGIMO University). “Northern Influence”. *Izvestia*. 17.03.2022. URL: https://iz.ru/1305812/nikita-lipunov/severnoe-vliianie
12. Mikhailichenko, D. “Without Russia : How Realistic Is the Scenario of Her Leaving the Arctic Council?”. *Go Arctic*. 8.07.2022. URL: https://goarctic.ru/politics/bez-rossii-realistichen-li-stsenariy-vykhoda-iz-arkticheskogo-soveta/
13. Riedel, A. et al. “What Future for Cooperation in the Arctic? Scenarios After Putin’s War on Ukraine” [in English]. *Blog of the German Institute of Development and Sustainability (IDOS)*. 16.03.2022. URL: https://blogs.idos-research.de/2022/03/16/what-future-for-cooperation-in-the-arctic-scenarios-after-putins-war-on-ukraine/
14. Rogoff, A. “It’s Time for an Arctic Council 2.0” [in English]. *Arctic Today*. 5.03.2022. URL: https://www.arctictoday.com/its-time-for-an-arctic-council-2-0/
15. Sukhoverkova, A. “Arctic Sessions : Science Diplomacy as the key to Reviving Cooperation in the Arctic”. *Go Arctic*. 13.08.2022. Citing Sergunin, A. (Professor at Saint-Petersburg State University) and Devyatkin, P. (Research Associate at The Arctic Institute) URL: https://goarctic.ru/politics/arctic-sessions-nauchnaya-diplomatiya-klyuch-k-vozrozhdeniyu-sotrudnichestva-v-arktike/
16. Viakhireva, N. (RIAC Program Manager). “On Pause: Dialogue with Russia in the Arctic” [in English], *Russian International Affairs Council: RIAC*. 20.04.2022. URL: https://russiancouncil.ru/en/analytics-and-comments/analytics/on-pause-dialogue-with-russia-in-the-arctic/

Improvement of sea ice thickness measurement method using the shipborne Electro-Magnetic Inductive device

Kosuke Kawamura[1], Kazutaka Tateyama[2]
[1] *Graduate School of Engineering, Kitami Institute of Technology*
[2] *Kitami Institute of Technology*

The Arctic sea ice extent has been rapidly decreasing since the late 1970s due to rising atmospheric and sea water temperatures associated with global warming, with the smallest sea ice extent ever recorded in September 2012. The salinity of seawater in the Arctic Basin is decreasing due to melting sea ice as well as increased freshwater supply from rivers (Krishfield et al., 2014).

This study estimates sea ice thickness using EM, since it has been reported that changes in seawater salinity affect the accuracy of EM (electromagnetic induction sensor) measurements. (Takahashi, 2016).

There is a marked conductivity difference between sea ice and seawater, and the EM method uses this difference to measure the apparent conductivity σa and estimate the distance ZE from the sensor to the sea ice bottom.(tateyama et al.2006)

In this study, data acquired during the Joint Ocean Ice Study (JOIS) 2010-2022, which takes place over one month out of 7-10 each year, are used in the analysis. The JOIS is conducted in the Beaufort Sea, Canada (Figure 1). Data used include total ice thickness obtained from EM and visual observations, GPS to determine observation locations, and electrical conductivity of navigated seawater. Then, based on the acquired data, we estimate it by 1D 3-layer model calculation (snow cover, sea ice, and sea water layer) using the numerical analysis program "PCLOOP".

Finally, we compare the total ice thickness (ZI). (Figure 3) The right side is before correction and the left side is after correction, and this result shows that the overall correction was small. This result was similar in other years as well.

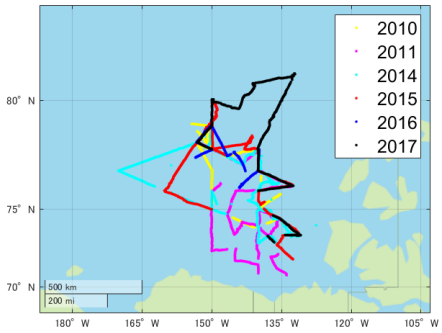

Figure 1. Passage during EM

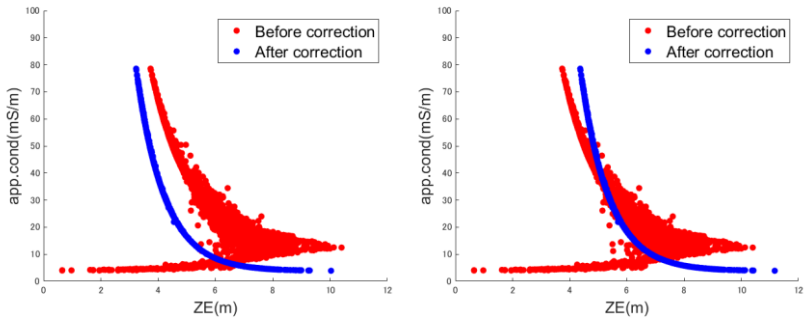

Figure 2. 2017's correction ZE

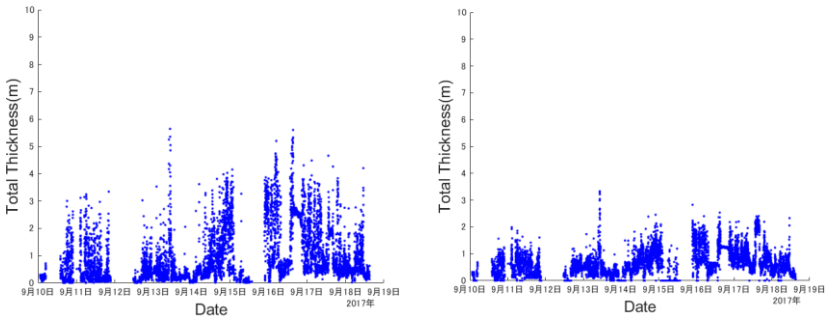

Figure 3. Before and after correction ZI

References

Krishfield, R. A. and 6 others (2014): Deterioration of perennial sea ice in the Beaufort Gyre from 2003 to 2012 and its impact on the oceanic freshwater cycle, J. Geophys. Res. Oceans, 119(2), 1271-1305,

Takahashi. S(2016),: Considering surface salinity by shipboard EM Sea Ice Thickness Measurement Method. Graduation thesis at Kitami Institute of Technology,43

Tateyama. K. and 5 others (2006): Standardization of electromagnetic-induction measurements of sea-ice thickness in polar and subpolar seas. Annals of Glaciology, 44(1): 240-246

Response of Eurasian Temperature to Barents–Kara Sea Ice: Evaluation by Multi-Model Seasonal Predictions

Kensuke Komatsu[1,2], Yuhei Takaya[1], Takahiro Toyoda[1], and Hiroyasu Hasumi[2]
[1]*Meteorological Research Institute, Japan Meteorological Agency*
[2]*Atmosphere and Ocean Research Institute, The University of Tokyo*

Barents–Kara(BK) sea ice anomaly (SIA) are considered a potential source of seasonal predictability in the midlatitudes, but confirmation or refutation of this possibility remains elusive. Especially controversial is the link to the Warm Arctic– Cold Eurasia (WACE) pattern. While the internal atmospheric variability (Ural high pressure system) drives both BK sea ice and WACE pattern, the reinforcing of WACE by sea ice is also argued. The resent study pointed out that the prediction of winter Eurasian surface temperature degraded when November BK sea ice conditions are not taken into account. To improve seasonal predictions, the contribution of sea ice forcing to the WACE pattern and model limitations need further investigation.
This study examined the interannual linkages between BK sea ice, winter Eurasian temperature, and WACE in hindcasts of state-of-the-art coupled seasonal prediction models. In addition, this study quantified the amplitudes of sea ice variability and its influence by the models. In the models analyzed, the WACE index is strongly depended on the BK temperature and did not rigorously reflect a sea ice–Eurasia causal link. The autumn BK sea ice anomaly was not a precursor of winter atmospheric conditions over Eurasia. Rather, the winter atmospheric circulation likely drives both winter BK sea ice and Eurasian temperature. However, the predicted winter sea ice–Eurasia links are likely weaker than the observed. This contrast is speciously related to the modest sea ice variance, but the actual influence of BK sea ice variation on Eurasian temperature anomalies is still questionable

References

Komatsu, K. K., Takaya, Y., Toyoda, T., & Hasumi, H. (2022). Response of Eurasian temperature to Barents–Kara sea ice: Evaluation by multi-model seasonal predictions. Geophysical Research Letters, 49, e2021GL097203. https://doi.org/10.1029/2021GL097203

Two new species of basidiomycetous yeast *Mrakia* sp. isolated from Ward Hunt Lake in the Canadian High Arctic

Masaharu Tsuji[1], Yukiko Tanabe[2, 3], Warwick F. Vincent[4], Masaki Uchida[2, 3]
[1] *National Institute of Technology, Asahikawa College*
[2] *National Institute of Polar Research*
[3] *The Graduate University for Advanced Studies (SOKENDAI)*
[4] *Université Laval*

Ward Hunt Lake is located on Ward Hunt Island, off the northern coast of Ellesmere Island at the northern limit of North America (83°05.226'N; 74°08.721'W). The lake is 0.37 km^2, of which the majority is shallow (i.e., <2 m), with a maximum depth of 9.7 m. Ward Hunt Lake is perennially ice-covered. However, the ice cover of Ward Hunt lake thinned from 2008 onward, and the lake became ice-free in 2011 (1,2).

In 2018, as part of a microbial survey in the lake, 3.3m depth of lake sediments were collected and transferred aseptically to sterile 5-mL sample tubes. Within one hour of sampling, the tubes were transferred to a –20°C freezer at the field laboratory and then stored at that temperature until subsequent analysis.

Subsamples (0.1 g) of the lake sediment were placed on potato dextrose agar (PDA; Difco, Becton Dickinson Japan, Tokyo, Japan) containing 50 μg/mL chloramphenicol and incubated at 10°C for a period of up to 3 weeks. We isolated fungi growing on the PDA based on colony morphology. Each colony with a different morphology was purified by repeated streaking on fresh PDA. DNA was extracted from fungal colonies using an ISOPLANT II kit (Wako Pure Chemical Industries, Osaka, Japan) according to the manufacturer's protocols. The extracted DNA was amplified by polymerase chain reaction (PCR) using KOD–plus DNA polymerase (Toyobo, Osaka, Japan). After that, the DNA was purified using Sephacryl S–400HR (Sigma-Aldrich Japan, Tokyo). Sequences were determined using an ABI Prism 3130xl Sequencer (Applied Biosystems, Life Technologies Japan, Tokyo).

A total of 102 fungal strains were isolated from the 2018 sediment samples. Based on the internal transcribed spacer (ITS) region and 26S rDNA D1/D2 domain sequence similarity, these strains were classified into 19 genera and 28 species. The dominant fungi belonged to the genera *Mrakia* (32.7%), *Vishniacozyma* (13.1%), and Pseudogymnoascus (9.3%).

Phylogenetic analysis of two strains showing low sequence homology with the ITS and D1/D2 regions. Result of the phylogenetic analysis, these two strains may be new species of the genus *Mrakia*. Further experiments will be conducted on these strains to propose them as new species, *Mrakia wardhuntensis* and *M. yamadae*.

References

1. Paquette, M.D. Fortier, D. R. Mueller, D. Sarrazin, and W. F. Vincent, Rapid disappearance of perennial ice on Canada's most northern lake, Geophys. Res. Lett., 42, 1433–1440, 2015.

2. Bégin, P.M, Rautio, Y Tanabe, M Uchida, A.I. Culley, W.F.Vincent, The littoral zone of polar lakes: Inshore-offshore contrasts in an ice-covered High Arctic lake., Arctic Sci. in press, 2020. https://doi.org/10.1139/AS-2020-0026

Co-occurrence patterns of soil microbial communities in the low Arctic tundra are affected by the vegetation coverage

Shu-Kuan Wong[1], Yingshun Cui[2], Seong-Jun Chun[3], Ryo Kaneko[1], Shota Masumoto[4], Ryo Kitagawa[5], Akira S. Mori[4], and Masaki Uchida[1,6]

[1] *National Institute of Polar Research, Research Organization of Information and Systems, Tachikawa, Tokyo.*

[2] *Division of Life Science & Plant Molecular Biology and Biotechnology Research Center, Gyeongsang National University, Korea*

[3] *LMO Research Team, National Institute of Ecology, Seocheon, Korea*

[4] *Graduate School of Environment and Information Sciences, Yokohama National University, Tokiwadai, Hodogaya, Yokohama.*

[5] *Kansai Research Center, Forestry and Forest Products Research Institute, Nagaikyutaroh, Momoyama, Fushimi, Kyoto.*

[6] *Department of Polar Science, School of Multidisciplinary Sciences, The Graduate University for Advanced Studies, SOKENDAI, Tachikawa, Tokyo.*

Global climate change is projected to increase the global temperatures, leading to stronger warming in the Arctic regions. Soil microbial communities are actively involved in the biogeochemical cycles in the Arctic region. However, continuous warming will most likely affect the distribution and functions of these microbial communities. This study investigates the soil bacterial community structure and diversity from three different areas with varying vegetation coverage and soil biogeochemical properties in the low Arctic tundra of Salluit and how the bacteria interacts with the different environmental parameters from these environments.

A total of 225 soil samples were collected randomly from three sites. The high elevation transect was set up at the top of the hill with low vegetation coverage, the mid elevation transect was set up mid-hill with intermediate coverage and the low elevation transect was set up in the lower slopes with high vegetation coverage. At each site, three 150 m transects, each situated 50 m apart, were set up at three different environmental conditions with low, intermediate, and high vegetation coverages, respectively. Twenty-five topsoil samples were collected using a sterile scoop from each transect at 6 m intervals and DNA was extracted from each sample. The V3-V4 region of bacterial 16S rRNA gene was amplified and sequenced using the Illumina MiSeq sequencer to determine the bacterial community composition. The resulting sequences were analyzed using QIIME2 pipeline. Microbial co-occurrence networks, structural equation modelling and subsequent statistical analysis were preformed using packages in R software.

Amplicon sequence variants (ASVs) obtained from our samples were categorized into generalist, common taxa and specialist based on their niche breadth index. We found differences within the three bacterial niches (specialist, common taxa and generalist) in terms of the bacterial composition and abundance. Based on detailed network analysis and structural equation modeling, these differences were mainly driven by the different environmental conditions. Plant coverage, especially those of vascular plants which are abundant in low elevation areas, were the main factor controlling the distribution of generalist and to a lesser extent, the common taxa. The distribution of generalist, in turn, controlled the distribution of common taxa. On the other hand, the distribution of specialist was affected by the common taxa but not plant coverage. In short, plant coverage controls the distributions of generalist, which in turn regulates the distribution of common taxa that controls the specialist at the sampling area. Generalists, mainly Rhizobiales, acts as bridges to connect the different microbial communities and assists the surrounding microbes. Specialists, dominated by Ktedonobacterales, on the other hand, only interacts mainly within the group and to a lesser extent, with the common taxa but not the generalist. This result suggested that specialist in the sampling area have a much smaller and limited niche and interacts among themselves to form a close-knit micro-environment to survive in the tundra area. Compared to the generalist and common taxa, these specialists formed a very close-knit and independent microbial cluster within a specific microenvironment; possibly as a strategy to help them persist and survive in the harsh tundra.

In short, we have shown that the distribution of generalist, common taxa and specialist were driven by different environmental factors and these groups have specific interactions among and within each other to help them thrive in the low Arctic. Our results have also revealed that there are complex plant-microbe interactions in the low Arctic tundra. Identifying and studying these interactions are particularly important as climate change will affect both vegetation and microbe; both of which that are particularly sensitive and vulnerable to changing temperatures.

Drone survey of Qaanaaq Glacier, northwestern Greenland, for precise DEM construction and for mapping supraglacial streams

Shinta Ukai[1,2], Shin Sugiyama[1], Ken Kondo[1,2]

[1]Institute of Low Temperature Science, Hokkaido University

[2]Graduate School of Environmental Science, Hokkaido University

Greenland is currently influenced by rapidly warming climate in the Arctic, which causes melt and retreat of glaciers situated along the coast. To better understand processes driving the glacier change, we have studied Qaanaaq Ice Cap in northwestern Greenland since 2012. As a part of the field campaign in the summer 2022, we conducted drone observations over Qaanaaq Glacier, an outlet glacier of the ice cap. The survey took place for seven days between July 14 and August 11. A drone (DJI phantom4pro V2.0) was operated at 120 m above the glacier to take images with a resolution of 33 mm per pixel, and with overlap of 70% to the flying direction and sidelap of 65%. Six painted wooden plates were distributed around the glacier and surveyed with kinematic GNSS positioning to improve the accuracy of the drone survey. Repeated surveys were carried out at elevation of 720 m a.s.l. over an area of 914000m^2 to monitor the change in the glacier surface features. 677 images were acquired during each of six surveys. The images clearly indicate the evolution of supraglacial streams, which are considered to be important for ice melt as well as glacier hydrology. Lower reaches of the glacier were surveyed on 10 August to generate a DEM covering an area of 1336000 m^2. The photographs were processed with software Metashape to generate an orthorectified mosaic image and construct a DEM with a resolution of 26 mm. This DEM will be compared with surface elevation data previously obtained by in-situ GPS survey and satellite remote sensing to quantify the mass loss of the glacier over the last decades.

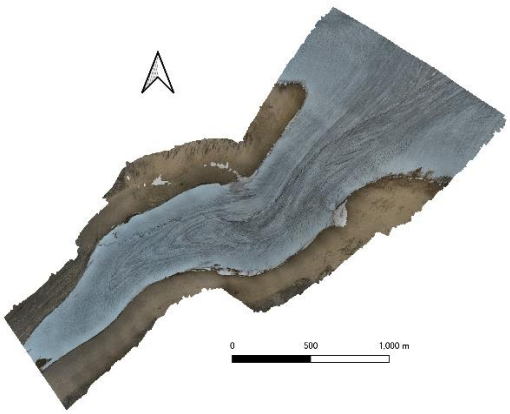

Figure 1. Orthorectified mosaic image of Qaanaaq Glacier.

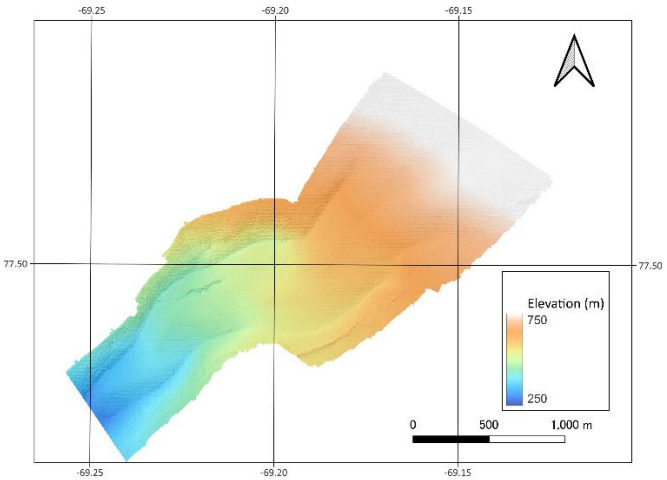

Figure 2. DEM of Qaanaaq Glacier constructed from the drone survey.

Changes in stripe patterns in dark regions on the southwestern Greenland Ice Sheet

Akane Uruma[1] and Nozomu Takeuchi[2]
[1]*Faculty of Science, Chiba University*
[2]*Graduate School of Science, Chiba University*

1. Introduction

On the Greenland Ice Sheet, the bare ice surface is exposed at the marginal parts of the ice sheet during summer. In the bare ice area, dark colored ice, called a dark region, appears at the same locations every year. The dark region expands particularly in the southwestern part of the ice sheet over a distance of about 500 km from north to south. In recent years, the area of the dark region has expanded. The expansion of the dark region reduces surface albedo of the ice sheet and promotes absorption of solar radiation, which accelerates melting of the ice and leads to loss of the ice sheet mass. Therefore, it is important to understand the factors that affect the area of the dark region. Field observations and satellite image analyses have shown that the dark region is formed by the deposition of light-absorbing impurities such as dust and snow/ice microorganisms on the ice surface. High-resolution satellite images show that the dark region consists of stripe patterns extending in parallel with the ice sheet margins. However, it is still unclear why dust and snow/ice microorganisms accumulate on the ice surface to form stripe patterns, and what is the relationship between the patterns and expansion of the dark region. The purpose of this study is to analyze the changes in stripe patterns of the dark region in the southwestern part of the Greenland Ice Sheet using satellite images, and to discuss the factors that cause the changes in the dark region.

2. Study site and methods

The bare ice area of the Greenland Ice Sheet can be divided into two areas, which are the white and dark regions. The white region is defined as the area where the surface appears to be bright and tends to distribute the downstream of the bare ice area. The dark region is defined as the area where the surface appears to be dark and tends to distribute the upstream of the bare ice area. Three Landsat-8 OLI satellite images acquired on 10-July, 26-July, and 11-August, in 2019, were used in this study. A transect line across the white and dark regions was selected to be analysed with satellite images. A profile of Band 2 reflectance along the transect line was obtained using a geographic information system application (QGIS).

3. Results and Discussion

The profile of reflectance along the transect line shows that the reflectance was mostly constant in the white region, while it largely varied in the dark region. Baced on the reflectance, the dark region was further divided into three areas: dark stripe, white stripe, and intermediate-stripe. The comparison of the reflectance profiles among the three images in July and August revealed that there was little change in reflectance in the white region while there was a significant change of reflectance in the dark region in July. In the dark region, the reflectance of intermediate-stripe particularly decreased but those of dark and white stripes decreased slightly. Results show that the change in reflectance of the bare ice surface varies from area to area : the reflectance did not changed in the white region, changed slightly in the dark and white stripes, and changed significantly in the intermediate-stripes in the dark region during the melting season. The reason for the significant decrease in reflectance in the intermediate-stripe may be due to the growth of microbes such as glacier algae promoted by more abundant nutrient supply from the ablating ice, and/or to the surface ice structure that aggregate surface impurities on the bare ice surface.

Recent activities of the ArCS II Research Infrastructure: Earth Observation Satellite Data

Rigen Shimada[1], Kazuki Nakata[1], Misako Kachi[1], Takeo Tadono[1], Hiroshi Murakami[1], Eri Yoshizawa[1] and Yukio Kurihara[1]
[1]*Earth Observation Research Center, Japan Aerospace Exploration Agency*

Japan Aerospace Exploration Agency (JAXA) participates in the Arctic Challenge for Sustainability II (ArCS II) Project as the Research Infrastructure: Earth Observation Satellite Data. Taking advantage of satellite observations as spatial and temporal wide coverage of the Arctic region, we play a role in providing observation data on the atmosphere, ocean, land, ecosystem and cryosphere from JAXA's Earth observation satellites in an easy-to-use format for researchers, in cooperation with the Arctic Data archive System (ADS) in National Institute of Polar Research (NIPR). In collaboration with ADS, we have been organizing satellite data requests, processing and providing data, and support for data analysis through the ArCS II project.

The GCOM-C/SGLI and GCOM-W/AMSR2 products are routinely processed and provide, and the quality of the products were continuously improved through version upgrades by evaluating product accuracy and improving algorithms. For example, all GCOM-C/SGLI standard products were major version upgraded twice in FY2020 and FY2021. Through these upgrades, these products were improved quality. GCOM-W/AMSR2 all standard products and several research products are continuously provided. The sea surface temperature product was major version upgraded in FY2020 and minor version upgraded in FY2022. The total precipitable water and cloud liquid water products were minor version upgraded in FY2021.

In addition, new research products are released to expand the use of new satellite observation data. Since the start of the ArCS II project, we have released new research products that contribute to the understanding of changes in the cryosphere or polar region environment, such as the AMSR2 high-resolution sea ice concentration (Fig. 1), AMSR2 sea ice motion vector, AMSR2 snow depth, AMSR2 soil moisture content and SGLI snow and ice surface albedo products (Fig. 2). These products are now preparing for easy browsing on the web in cooperation with ADS. In this context, we also developed the format conversion tool to convert satellite data into user-friendly formats such as netCDF and GeoTIFF.

We also provided analysis support in response to requests received from the ArCS II researchers. In FY2021, we conducted interferometric SAR (InSAR) processing using ALOS-2 data for permafrost areas and provided them.

From this fiscal year, we have been conducting interview surveys for each Research Programs promoted by the ArCS II project in order to further expand the use of satellite data that may support their research activities. Based on the understanding of the status of data use, we are investigating the problems that researchers have in using satellite data and identifying and analyzing the factors that hinder the expansion of data use.

In the second half of the ArCS II project, we will continue to provide the satellite observation data, evaluate the product accuracy, improve algorithms, and release new research products. In addition, in order to solve the issues identified based on the interview surveys, we will develop manuals and tutorials for satellite observation data handling as user-friendly formats. Through these activities, we aim to further expand the use of earth observation satellite data in Arctic research.

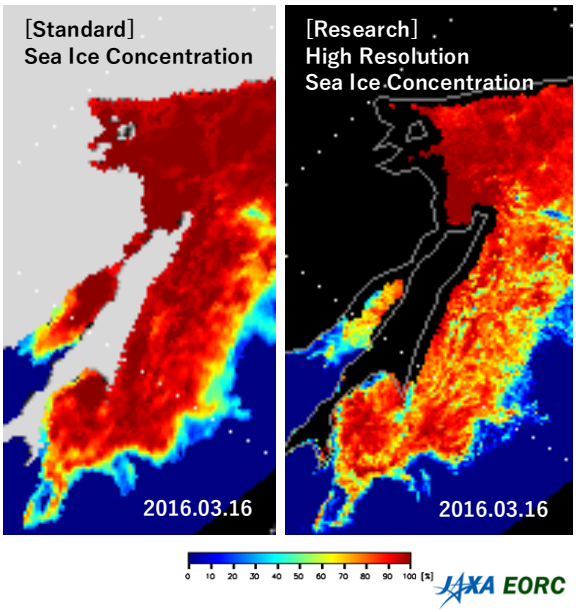

Fig. 1 Comparison between AMSR2 sea ice concentration as a standard product (left) and high-resolution sea ice concentration as a research product (right).

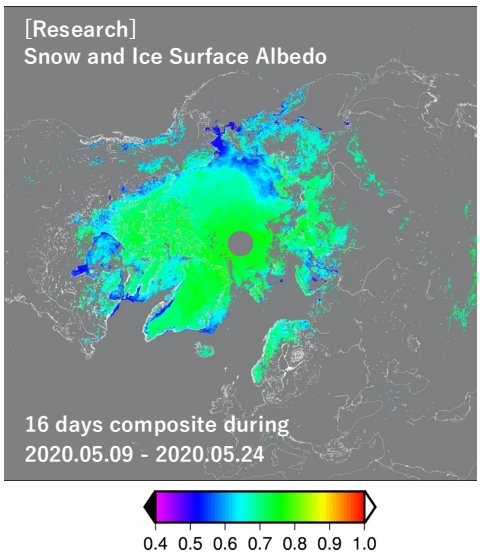

Fig. 2 Snow and ice surface albedo distribution in the northern hemisphere derived from SGLI.

Testing of alternative data for generating the JASMES long-term snow cover extent product

Masahiro Hori[1], Masashi Niwano[2,4], Rigen Shimada[3,2], Teruo Aoki[4,2]

[1]*University of Toyama*
[2]*Meteorological Research Institute*
[3]*Japan Aerospace Exploration Agency*
[4]*National Institute of Polar Research*

Snow cover is an important geophysical variable to be observed from space for monitoring the effect of the global warming on the Arctic region. We have been producing the JASMES long-term global snow cover extent (SCE) data derived from two satellite-borne optical imagers, Advanced Very High Resolution Radiometer (AVHRR) and Moderate Resolution Imaging Spectroradiometer (MODIS) and have revealed the occurrence of the significant negative trends of annual snow cover duration in the western Eurasian continents during the past four decades (Hori et al., 2017). The operation of MODIS sensors used for the SCE generation have continued for more than 20 years and thus the use of alternative sensors should be considered for preparing future sensor failure. A candidate of the alternative sensors is the Visible Infrared Imaging Radiometer Suite (VIIRS) onboard US's Suomi-NPP satellite and JPSS series satellites. In this study, we examined the applicability of Suomi-NPP/VIIRS data for the long-term SCE generation. VIIRS has the same spectral bands as AVHRR and MODIS used for the JASMES SCE analysis and thus the same algorithm can be employed with some adjustments of radiance taking into account the difference in spectral responses. The analysis results showed that the SCEs derived from VIIRS data are consistent well with those derived from the data of MODIS on Aqua satellite within the error of 3% as shown in Figure 1. Therefore, VIIRS can be a good alternative sensor of MODIS on Aqua for extending the long-term record of SCE toward the future.

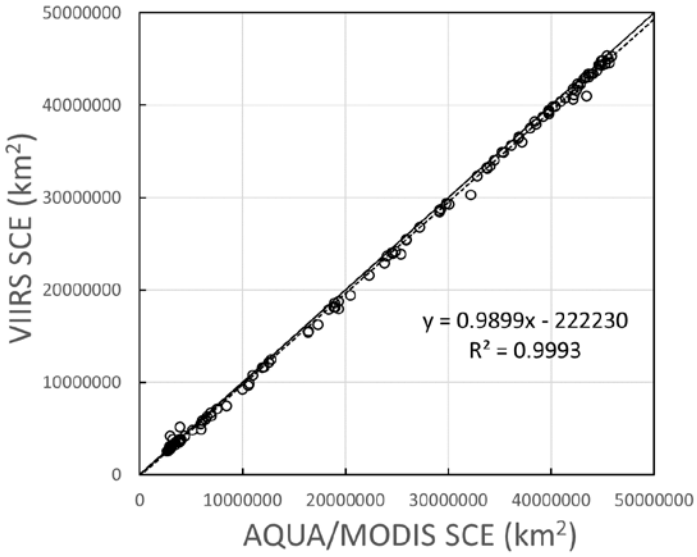

Figure 1. Comparison of the Northern Hemisphere snow cover extents derived from MODIS on Aqua satellite (AQUA/MODIS SCE) and those derived from VIIRS (VIIRS SCE) for the period of 2017-2022 (5 years).

References

Hori, M., K. Sugiura, K. Kobayashi, T. Aoki, T. Tanikawa, K. Kuchiki, M. Niwano and H. Enomoto, A 38-year (1978–2015) Northern Hemisphere daily snow cover extent product derived using consistent objective criteria from satellite-borne optical sensors, Remote Sensing of Environment, 191, 402-418, https://doi.org/10.1016/j.rse.2017.01.023, 2017.

Fast computation of Arctic Sea Route Search Systems using GPUs

Takeshi Sugimura[1], Hironori Yabuki[1] and Hajime Yamaguchi[1]
[1]*National Institute of Polar Research*

A container ship stranding accident occurred in the Suez Canal in March 2021. This blocked traffic in the canal, and it took ten days for congestion to ease. This incident pointed out the danger of the concentration of the transportation network, and the Northern Sea Route (NSR) attracted attention as an alternative transportation method to decentralize the transportation network.

In the case of the NSR, it is essential to ensure a safe route to determine the shipping route based on the icebreaking capacity of the vessel and the sea ice conditions. If the ship is operated incorrectly, a collision with the ice could cause a serious accident. At present, such decisions depend on the experience of the crew. However, there are few opportunities to gain onboard expertise in sea ice areas. Therefore, training using actual routes is required, as in the exercises on the map, to complement the experience. In addition to training, safer navigation would be possible if the support system supports secure and efficient navigation. Establishing a ship navigation support system for sea ice areas is an urgent issue for the development of the NSR.

This study has developed an Arctic Sea Route Search System that automatically calculates safe and efficient routes. This system is developed and published as a web application, so that necessary data can be automatically obtained from the network and can calculate the optimal route according to the vessel's capabilities. The system is designed so that anyone can quickly get the optimal route by operating the GUI on the screen. The program uses the Ice Index method to estimate ship speed and the route search method to find the optimal route. By using GPUs to perform some of the calculations, calculations can be performed 3.75 times faster on average and up to 7.04 times faster than with conventional systems. The validity of the system was verified by comparison with AIS data. This clarified issues to be considered in the future.

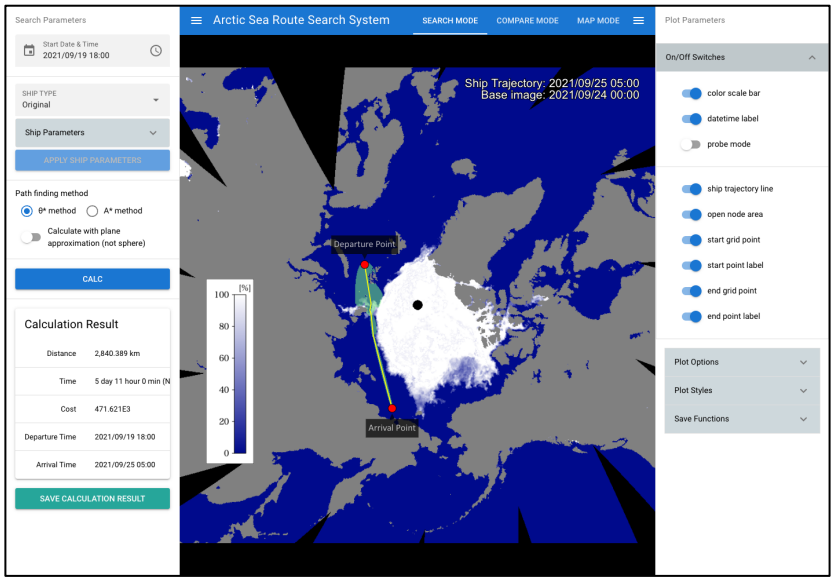

Figure 1. Web application of arctic sea route search system on the ADS web site.

Educational Practices using Polar Sea Ice Data for High School Science and Mathematics Classes

Yoshihiro Niwa[1], Takashi Ishibashi[2], Akiko Mohri[1] and Hironori Yabuki[1]
[1]*Arctic Environment Research Center, National Institute of Polar Research*
[2]*Secondary School attached to the Faculty of Education, the University of Tokyo*

Climate change education is essential for the next-generation of young students who will be directly affected and must cope with its threats in the future. For these students, it is important to have an experience processing and closely observing real-world climate data to promote a data-based discussion. As an example of the data-based climate change education, we conducted two different classroom practices using actual polar sea ice data for high school students. Polar sea ice data are suitable for this educational purpose, since Arctic sea ice shows the clearest global warming signal. In addition, all students can guess and discuss the ice melt/formation process based on their daily experiences.

The first educational practice was conducted in February 2018 at secondary school attached to the faculty of education of the university of Tokyo for 36 first-grade high school students in their two-hour mathematics class on data analysis. In this class, each student used a desktop computer to analyze the 5-day-interval Arctic and Antarctic sea ice extent data for 30 years (1979-2008). For most of the students, this was their first experience processing large data from the real world. They drew the sea ice extent graphs using Microsoft Excel and added regression lines (Figure 1). Then, they compared the change in sea ice extent in the Arctic where a clear downward trend can be confirmed with that in the Antarctic where the regression line shows a slight upward trend. This result was contrary to their expectations, as they expected that the sea ice extent both in the Arctic and Antarctic would decrease with global warming. Then, they had a free discussion about global warming, the Arctic and Antarctic climates, and the validity of the data analysis results.

The second educational practice was conducted in October 2022 at Tokyo metropolitan Tachikawa high school for 42 first-grade high school students in their two-hour science class on scientific inquiry activity. We aimed for students to motivate an active attitude toward observing scientific data. The satellite-derived Arctic sea ice concentration data (Figure 2) visualized and provided by the Arctic data archive system (ADS) (https://ads.nipr.ac.jp/vishop/#/monitor) of NPRI (National Institute of Polar Research) were used in this class. First, we explained how to access and operate the ADS homepage. Then, each student operated ADS with a laptop computer to repeatedly and closely observe the seasonal variation in the Arctic sea ice concentration field. To promote their close observation, we asked the students the following question “What do you notice from the data? Please answer one thing for each person. Anything is OK, but answer different thing from what the others have answered.”. Figure 3 shows the whiteboards that list the answers received in the class. We can confirm that the students had noticed, shared, and learned a variety of characteristics of sea ice, ocean, and geography in the Arctic region.

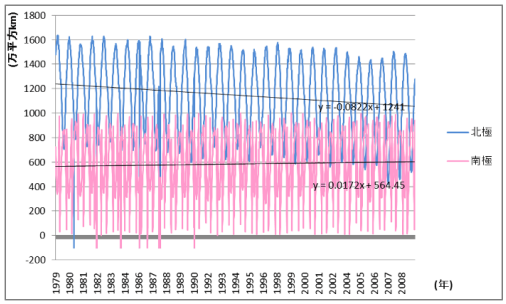

Figure 1. The Arctic and Antarctic sea ice extent graphs drawn in the first educational practice.

Figure 2. The example of the ADS data used in the second educational practice

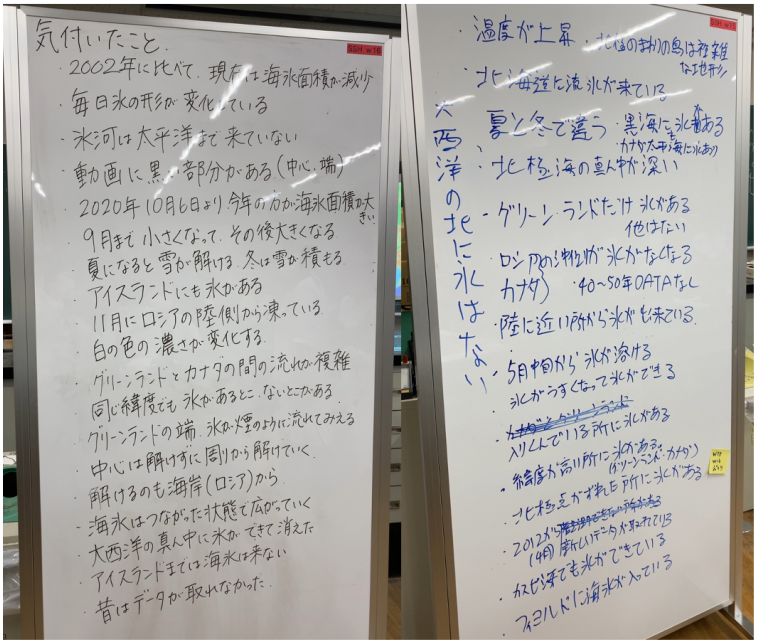

Figure 3. The whiteboards in the second educational practice that list what the students noticed from the ADS data.